PrimPol bypasses UV photoproducts during eukaryotic chromosomal DNA replication

Julie Bianchi[1†], Sean G. Rudd[1†], Stanislaw K. Jozwiakowski[1], Laura J. Bailey[1], Violetta Soura[1], Elaine Taylor[2], Irena Stevanovic[3], Andrew J. Green[1], Travis H. Stracker[3], Howard D. Lindsay[2], Aidan J. Doherty[1*]

[1] Genome Damage and Stability Centre, School of Life Sciences, University of Sussex, Brighton, BN1 9RQ, UK.

[2] Lancaster Medical School, Faculty of Health and Medicine, Lancaster University, Lancaster, LA1 4YQ, UK.

[3] Institute for Research in Biomedicine (IRB Barcelona), Barcelona, 08028, Spain.

[†] Contributed equally to this work

[*] To whom correspondence should be addressed. Email: AJD21@sussex.ac.uk

Running title: PrimPol bypasses UV lesions at replication forks

SUMMARY

DNA damage can stall the DNA replication machinery leading to genomic instability. Thus, numerous mechanisms exist to complete genome duplication in the absence of a pristine DNA template, but identification of the enzymes involved remains incomplete. Here, we establish Primase-Polymerase (PrimPol; CCDC111), a novel archaeal-eukaryotic primase (AEP) in eukaryotic cells, is involved in chromosomal DNA replication. PrimPol is required for replication fork progression on ultraviolet (UV) light damaged DNA templates, possibly mediated by its ability to catalyze trans-lesion synthesis (TLS) of these lesions. This PrimPol UV lesion bypass pathway is not epistatic with the Pol η-dependant pathway and, as a consequence, protects xeroderma pigmentosum variant (XP-V) patient cells from UV-induced cytotoxicity. In addition, we establish that PrimPol is also required for efficient replication fork progression during an unperturbed S-phase. These, and other findings, indicate that PrimPol is an important player in replication fork progression in eukaryotic cells.

INTRODUCTION

DNA damage frequently stalls the DNA replication machinery and therefore bypass mechanisms exist to ensure complete chromosomal duplication and prevent genome instability (Aguilera and Gómez-González, 2008). DNA Replication can restart directly at stalled replication forks using low-fidelity DNA polymerases that catalyze translesion synthesis (TLS; Sale et al., 2012) or by homologous recombination (HR), which utilizes an alternative undamaged sister template to allow extension of the stalled primer terminus (Li and Heyer, 2008). DNA replication can also proceed in the presence of damage by convergence of adjacent replicons, discontinuous synthesis of Okazaki fragments on the lagging strand, or re-priming of DNA synthesis downstream of lesions on the leading strand (Heller and Marians, 2006; Yeeles and Marians, 2011). These produce single-stranded (ss) DNA gaps behind replication forks that are subsequently filled using TLS or HR (Lopes et al., 2006). Although our understanding of damage tolerance processes is advancing, identification of enzymes involved in these pathways is not yet complete. Eukaryotic cells employ a number of distinct DNA polymerases for propagation of chromosomal DNA, but only one archaeo-eukaryotic primase (AEP), Prim1, has been described as requisite (Frick and Richardson, 2001). Whilst AEPs were once considered to solely prime DNA synthesis, it is now evident that AEPs have additional biological functions, exemplified by their role in prokaryotic DNA break repair (Della et al., 2004; Pitcher et al., 2007). Here, we establish that a second AEP is present in human cells, PrimPol (CCDC111), which can initiate DNA and RNA synthesis *de novo* and elongate existing DNA chains. Furthermore, we investigate cellular roles of PrimPol and establish that this novel AEP is required for efficient fork progression during chromosomal DNA replication on both damaged and undamaged templates in higher eukaryotes.

RESULTS

To determine if additional AEPs reside in the eukarya, a bioinformatics search was undertaken of the available eukaryotic genomes for genes with homology to AEP-like primases. In addition to the replicative primase, Prim1, we detected a second novel AEP-like gene/protein in eukaryotes, called CCDC111 (FLJ13366), previously reported to be a putative AEP superfamily member (Iyer et al., 2005). Following primase nomenclature, we named this enzyme PrimPol (Primase/Polymerase) to reflect its intrinsic biochemical activities (see below). PrimPol is present across the majority of eukaryotic species, from the earliest unicellular organisms (protists and algae) to plants, animals, and mammals, whilst some lower eukaryotes encode multiple PrimPol homologues. However, it is absent from prokaryotes, archaea, drosophila, all but one fungal species and *C. elegans*.. PrimPol contains two discernable motifs (Figure 1A), an N-terminal AEP catalytic domain and a C-terminal zinc finger similar to the viral UL52 primase domain.

To determine the activities encoded by human CCDC111, we over-expressed recombinant PrimPol in *E. coli* and purified it to near homogeneity (Figure S1A). To test if it possessed DNA/RNA primase activity, we incubated PrimPol with homopolymeric ssDNA, nucleotides (NTPs or dNTPs) and magnesium. PrimPol synthesized primers in the presence of either NTPs or dNTPs on a poly(dT) template (Figure 1B), consistent with the requirement of eukaryotic AEPs for templated pyrimidines to catalyse di-nucleotide synthesis (Frick and Richardson, 2001). Notably, dNTPs were utilized with a much greater efficiency than NTPs (Figure 1B). Mutation of the conserved active site metal binding residues (motif I: D114A, E116A; AxA) ablated priming activities (Figure 1B). Thus, PrimPol has robust DNA-dependent DNA and less prominent RNA primase activity, which is unique for eukaryotic primases. Although the eukaryotic replicative AEPs are dedicated DNA primases, some bacterial and archaeal AEPs are also DNA polymerases (Bocquier et al., 2001; Lipps et al., 2003; Della et al., 2004). To test if PrimPol has any associated DNA polymerase activities, the enzyme was incubated with a template-primer DNA substrate, dNTPs and magnesium. PrimPol readily extends the primer strand in a template-dependent manner in the presence of dNTPs (Figure 1C). The active site mutant also lacked polymerase activity (Figure 1C), confirming that both priming and extension activities are catalyzed by the same active site. To reflect the capacity of this novel enzyme to catalyze both DNA-dependent RNA/DNA primase and DNA polymerase activities, it was renamed PrimPol.

As bacterial AEPs are involved in DNA repair processes (Della et al., 2004; Pitcher et al., 2007), we assayed PrimPol for DNA lesion bypass activity. PrimPol efficiently bypassed

8-oxo-guanine lesions (Figure S1B), incorporating dA or dC with equal efficiency (Figure S1C), but was incapable of incorporating nucleotides opposite templated abasic or thymidine glycol lesions (Figure S1B). PrimPol was incapable of reading-through a templated *cis-syn* thymine-thymine (T-T) cyclobutane pyrimidine dimer (CPD) (Figure S1B), an ultraviolet (UV) photo-lesion that is a potent block for cellular replicases (Figure S1D). However, PrimPol was capable of extending a primer terminus with two dA residues annealed opposite the T-T CPD, with an efficiency comparable to an undamaged TT (Figure 1D). In contrast, human Pol ε or an archaeal PolB replicase were incapable of extending this primer terminus annealed to a CPD (Figure S1E). UV light also generates T-T pyrimidine-pyrimidone photoproducts (6-4 PPs) in DNA, which are highly distorting and cannot be efficiently bypassed by any individual mammalian DNA polymerase *in vitro*. Although both Pol ε and PolB stalled at this lesion (Figure S1F), strikingly, PrimPol could incorporate opposite and extend from a templated 6-4 PP (Figure 1E). Single incorporation assays revealed that PrimPol-dependant bypass was error-prone, incorporating dT opposite the 3' T, and dG or dC opposite the 5' T of the photoproduct (Figure 1F). Incorporation of dT opposite the 3' T of a 6-4 PP may be a distinct mechanism employed by PrimPol to facilitate bypass, as primer extension was only observed in the presence of the 6-4 PP (Figure 1G). Together, these data establish that PrimPol is a competent TLS polymerase, bypassing specific oxidative and UV-induced DNA lesions.

To establish the cellular localization of PrimPol, immunofluorescence (IF) detection of stably expressed PrimPol in HEK293 cells (Figure S2A-C) or endogenous PrimPol in 143B cells (Figure S2D) showed that it was predominantly cytoplasmic, although a small portion of this protein appeared nuclear. As PrimPol can bypass UV-induced DNA lesions *in vitro*, we next examined the sub-cellular localisation of PrimPol in UV irradiated cells. Cells stably expressing PrimPol were exposed to UV-C radiation and detergent-extracted prior to IF analysis. PrimPol re-localised to detergent-resistant sub-nuclear foci following UV-C irradiation (Figure 2A), numbering between 50 to several hundred per cell (Figure 2B) and the proportion of cells containing PrimPol foci was UV-C dose-dependent (Figure 2C). Foci were also observed following nucleotide deprivation by hydroxyurea (HU) treatment (Figure 2A), however this re-localisation of PrimPol was not a general response to DNA damage as no focal accumulation was observed following treatment of cells with ionising radiation (IR) (Figure 2A), which induces DNA strand breaks. To confirm that UV-C induced PrimPol foci represented sites of chromatin association, the detergent-insoluble chromatin fraction was prepared from UV-C irradiated cells and treated with DNase. This treatment successfully solubilized mono-ubiquitinated PCNA, present at replication forks stalled at UV photoproducts (Kannouche et al., 2004), and also released PrimPol into the soluble fraction (Figure 2D). Endogenous PrimPol in normal human fibroblasts also re-localises following UV-C irradiation,

partitioning to the detergent-insoluble chromatin-enriched fraction (Figure 2E). Together, these data support a role for PrimPol in the cellular response to UV-C radiation.

Defects in the bypass of UV photoproducts during chromosomal DNA replication result in activation of the intra-S phase checkpoint due to replication fork stalling. This is particularly evident in xeroderma pigmentosum variant (XP-V) cells (Bomgarden et al., 2006; Despras, et al., 2010), which lack the CPD TLS polymerase Pol η (Johnson et al., 1999; Masutani et al., 1999). As PrimPol bypasses 6-4 PPs and extends from CPDs, in addition to being a primase with a possible role in re-priming downstream of lesions, we hypothesised that it may function in a novel damage tolerance pathway that is complementary to Pol η. Therefore, the effects of depleting PrimPol in normal and XP-V cells treated with UV-C were investigated. RNAi treated cells were UV-C irradiated and, following recovery, analysed for detergent-resistant RPA foci and activation of the intra-S phase checkpoint kinase Chk1. These RPA foci are indicative of RPA-coated ssDNA present at stalled replication forks and, consistent with a requirement for PrimPol to bypass UV photoproducts, a significant increase in focal cells was observed in PrimPol-depleted fibroblasts (Figure S2E). Concurrently, an increase in phosphorylated Chk1 (S345) was also observed (Figure 2F), indicating activation by the replication stress response kinase, ATR. As bypass of UV photoproducts is already substantially impaired in XP-V cells, no further increase in RPA focal cells was observed in PrimPol-depleted XP-V cells (Figure S2E). However, Chk1 activation remained elevated 24 hours after irradiation with a low UV-C dose (Figure 2F), indicating a persistent defect in UV photoproduct bypass in the absence of both PrimPol and Pol η. In accordance with this, we observed ~5-fold increase of chromatin-bound Rad51 (Figure S2F) indicative of increased HR-mediated rescue of stalled replication forks in the absence of both PrimPol and Pol η. Despite PrimPol's role in the tolerance of UV photoproducts, PrimPol-depleted normal fibroblasts did not present any major UV-C sensitivity and, similarly, XP-V cells were only mildly sensitive to UV-C irradiation (Figure 2G). However, PrimPol depletion in XP-V cells rendered them synergistically sensitive to UV-C irradiation, decreasing the surviving fraction by up to a factor of 4 (Figure 2G). XP-V cells show greater sensitivity to UV when treated with low doses of caffeine (Arlett et al., 1975). To determine if this was due to inhibition of PrimPol, we repeated UV colony survivals on XP-V cells in the presence of 0.38 mM caffeine. Both XP-V cells and those depleted for PrimPol were more sensitive to UV than in the absence of caffeine (Figure S2G), suggesting that PrimPol is not the source of caffeine sensitivity in XP-V cells. To establish if PrimPol plays any roles in nucleotide excision repair (NER), we depleted PrimPol in NER deficient XP-A cells and observed an increase in UV sensitivity (Figure S2H), indicating that PrimPol's primary role is not in NER. Together, these findings establish that PrimPol operates in a UV lesion tolerance

pathway that is non-epistatic with Pol η and that this pathway protects XP-V cells from UV-C cytotoxicity by compensating for the loss of Pol η.

Next, we used avian DT40 cells to further investigate the role of PrimPol in the tolerance of UV-C induced DNA damage. PrimPol knockout (PrimPol$^{-/-}$) DT40 cells were viable (Figure S3A-C) and exhibited only minor proliferative (Figure S3D) and cell cycle defects, with a delayed G2/M transit (Figure S3E). Consistent with PrimPol's proposed role in the tolerance of UV photoproducts, PrimPol$^{-/-}$ cells were sensitive to low-doses of UV-C radiation and the UV mimetic 4-nitroquinoline 1-oxide (4NQO), in a similar manner to Pol η$^{-/-}$ cells (Figure 3A and B), but were not sensitive to IR (Figure 3C). Expression of human PrimPol in PrimPol$^{-/-}$ cells (Figure S3F) partially rescued both UV-C and 4NQO sensitivities (Figure 3A and B).

TLS-mediated damage tolerance can occur either at replication forks or in a post-replication manner. To determine the timing of PrimPol-mediated damage tolerance, the ability of PrimPol$^{-/-}$ cells to perform TLS post-replicatively on daughter strand gaps, was assessed using alkaline sucrose sedimentation analysis of nascent DNA in UV-C irradiated cells (Lehmann, 1972). As expected, a post-replication repair defect was observed in Pol η$^{-/-}$ cells but no defect was observed in PrimPol$^{-/-}$ cells (Figure 3D). This suggests that PrimPol is not required for post-replicative bypass of UV photoproducts. We next asked whether PrimPol is required to bypass UV photoproducts directly at stalled replication forks by analysing DNA fibre spreads. Notably, in the absence of UV-C irradiation, overall replication fork speeds were reduced in PrimPol$^{-/-}$ cells by ~20% (Figure S3G), and a similar reduction in DNA replication was observed by monitoring incorporation of radiolabelled thymidine (Figure S3H), suggesting a role for PrimPol during unperturbed chromosomal DNA replication. To analyse fork progression on UV damaged DNA, PrimPol$^{-/-}$ cells were exposed to UV-C radiation between thymidine analogue CldU and IdU labelling periods and the ratios between the two labels were calculated. In mock-irradiated cells, this ratio was ~1 (data not shown) however, following UV-C irradiation, this ratio increased significantly due to shortening of the second track indicating an impediment in replication fork progression. Compared to wild-type cells, PrimPol$^{-/-}$ cells showed a substantial increase in the spread and mean of CldU:IdU ratios (Figure 3E and F), indicating a marked increase in delay or blockage of replication fork progression on DNA containing UV photoproducts. In line with this, a reduction of radiolabelled thymidine incorporation was observed in PrimPol$^{-/-}$ cells compared to wild-type cells at varying UV-C doses (Figure S3I). Together, these data demonstrate that PrimPol is required for efficient replication of UV damaged chromosomal

DNA *in vivo*, which is consistent with the ability of PrimPol to extend from CPDs and bypass 6-4 PPs *in vitro*.

The proliferative, cell cycle, and DNA replication defects observed in PrimPol$^{-/-}$ cells (Figure S3) strongly support an additional role for PrimPol in normal S-phase. To explore this further, we examined PrimPol's localisation on chromatin during a synchronous round of DNA replication in *Xenopus* cell-free egg extracts. Recombinant human PrimPol became bound to chromatin during an unperturbed S-phase and this binding was abolished when replication was inhibited prior to initiation by geminin or the CDK inhibitor roscovitine (Figure 4A). By blocking elongation with aphidicolin treatment, increased chromatin-bound PrimPol was observed (Figure 4A), and again, abrogated by pre-treatment with geminin (Figure 4B). Similarly, endogenous PrimPol in normal human fibroblasts partitioned to the detergent-insoluble chromatin-enriched fraction following aphidicolin treatment (Figure S4A-B). Together, these data indicate PrimPol loads onto chromatin in a replication-dependent manner and this chromatin-association is even more apparent following replication fork stalling. Finally, we generated PrimPol$^{-/-}$ mice and subsequently mouse embryonic fibroblasts (MEFs) lacking expression of the PrimPol gene (Figure S4C-F), and analysed metaphase chromosome spreads. We observed an increase of metaphase aberrations in MEFs lacking PrimPol, in particular chromatid breaks (Figure 4C), which are indicative of lesions arising during S-phase. Further, following a prolonged treatment with low-dose aphidicolin, the percentage of metaphase aberrations increased substantially (Figure 4C). This supports a role for PrimPol in protecting replication forks from replication stress, which would be consistent with the aphidicolin and HU induced chromatin binding of PrimPol observed previously. Whether this role is re-initiation of DNA synthesis *de novo*, or akin to the role of Y-family polymerases during replication stress (de Feraudy et al., 2007; Godoy et al., 2006; Bétous et al., 2013) remains to be established.

DISCUSSION

Here, we extend the cellular role of AEPs, previously shown to function in initiation of DNA replication (Frick and Richardson, 2001) and prokaryotic DNA break repair processes (Della et al., 2004; Pitcher et al., 2007), by uncovering a function in bypassing UV lesions during chromosomal DNA replication in eukaryotic cells. There are at least two possible mechanisms of PrimPol-mediated fork progression (Figure 4D). With regards to damaged DNA templates, such as those containing UV lesions, PrimPol is a flexible DNA polymerase and thus can extend from a blocked primer terminus by directly synthesising across the lesion. PrimPol is also a primase, and therefore has the capacity to initiate DNA synthesis *de novo* downstream of the lesion following fork stalling, producing a ssDNA gap in the daughter strand. Presumably, the latter process would be restricted to lesions on the leading strand as discontinuous synthesis of Okazaki fragments on the lagging strand is inherently tolerant of DNA lesions (Svoboda and Vos, 1995; Pagès and Fuchs, 2003). Evidence of re-priming downstream of UV photoproducts exists in mammalian cells (Lehmann, 1972; Elvers et al., 2011), and most convincingly, in budding yeast, ssDNA gaps in the leading strand have been visualised behind replication forks in UV irradiated NER-deficient cells (Lopes et al., 2006). However, as PrimPol is absent from the majority of fungi, including budding yeast (Iyer et al., 2005), this re-priming is likely dependent upon the replicative DNA primase (Pri1) of the Pol α complex. Similarly, in *E. coli*, in which leading strand re-priming has been mechanistically described *in vitro*, the replicative DnaG primase is required for this process (Heller and Marians, 2006; Yeeles and Marians, 2011). By extrapolation, this suggests that if PrimPol re-primes downstream of leading strand lesions, it may function redundantly with the Pol α complex. Studies in *Xenopus* have demonstrated the Pol α complex is responsible for the bulk of primer synthesis at stalled replication forks (Michael et al., 2000; Van et al., 2010), although this may reflect the abundance of primers on the lagging versus leading strand. In support of PrimPol-mediated TLS, a number of studies have reported a common mis-insertion of dT opposite the 3' T of a 6-4 PP *in vivo*, with the polymerase involved remaining unidentified (Hirota et al., 2010; Szuts et al., 2008), suggesting that PrimPol may be responsible for incorporation opposite a subset of these lesions. PrimPol's ability to catalyse TLS opposite 6-4PPs could be particularly important, as they pose a significant block to replicases. Interestingly, the nuclear replicase Pol δ has been reported to incorporate two dA residues opposite a T-T CPD *in vitro* under certain circumstances (Narita et al., 2010; O'Day et al., 1992), and therefore PrimPol may function in concert with the cellular replicases to bypass CPDs. We also establish that PrimPol functions during unperturbed chromosomal DNA replication. PrimPol may be required for the bypass of naturally occurring DNA lesions or structures either by re-priming or as previously described for TLS polymerases (Bergoglio

et al., 2013). Regardless of the mechanism of PrimPol-assisted fork progression, it is evident that this novel AEP is an important new player at stalled replication forks in eukaryotic cells.

EXPERIMENTAL PROCEDURES

Protein preparation and activity assays

Human PrimPol cDNA was sub-cloned into pET28a (NdeI, BamHI) and the catalytic null mutant obtained by site directed mutagenesis. Both proteins were expressed in *E. coli* BL21 and purified with Ni^{2+}-NTA (Qiagen) followed by heparin and size-exclusion (GE Healthcare) chromatography columns. Primer extension assays were performed with 5' Hexachlorofluorescein labelled DNA primers (ATDbio). *De novo* DNA synthesis in the primase assay was detected by FAM-6-dATP (Jena-Biosciences) labeling of reaction products. Further detail of protein preparation, primer extension assays, and the fluorescent primase assay are detailed in the supplementary experimental procedures.

Mammalian cell culture and RNA interference

143B, HEK-293 Flp-In™ T-REx™ (Invitrogen) and MEFs were cultured in DMEM supplemented with 10% fetal calf serum (FCS), and SV40-transformed MRC5, XP30RO and XPA cells were cultured in MEM supplemented with 15% FCS. All cells were grown in 1% L-glutamine and 1% PenStrep. Generation of the HEK-293 Flp-In™ T-REx™ stable cell lines is detailed in the supplementary experimental procedures. Transfection of 10 nM PrimPol siRNA (5' -GAGGAAACCGUUGUCCUCAGUGUAU-3' , 5' -AUACACUGAGGACAACGGUUUCCUC-3') was performed using Lipofectamine 2000 (for 143b cells) or Lipofectamine RNAiMAX (Invitrogen) according to manufacturer recommendations.

Immunofluorescent analysis and cellular fractionation

For immunofluorescent analysis rabbit anti-PrimPol antibody (generated in house) was diluted 1:200, anti-RPA2 (Cell Signalling) 1:200, and anti-RAD51 (Abcam) 1:400. Cellular fractionation protocol was adapted from Kannouche et al., 2004. Further details are provided in supplementary experimental procedures.

Clonogenic survival assay

MRC5, XP30RO and XPA cells were either mock or PrimPol siRNA transfected, both at seeding and 24 hours after. At 72 hours dilutions of the transfected cells were plated in triplicate on 10 cm dishes. The next day the media was removed and cells were washed with PBS and then UV-C irradiated in the presence or absence of caffeine (0.38mM). After irradiation media was replaced and colonies allowed to grow over 10 days, before fixing with 100% ethanol and staining with methylene blue to allow counting.

Generation of PrimPol knockout avian DT40 cells and DNA replication/repair assays

Avian PrimPol gene was disrupted with histidinol and puromycin targeted cassettes following procedure described previously (Sonoda et al., 1998). Human PrimPol cDNA was sub-cloned into TET inducible vector (adapted from Clontech) containing luciferase gene reporter for clone selection. Further details in supplementary experimental procedures. DNA fibre analysis and the post-replication repair assay were performed as previously described (Edmunds et al., 2008). Post Replication Repair protocol was adapted to measure total DNA replication rate following UV-C, by pre-labeling cells with ^{14}C thymidine over two doubling time to normalize the amount of total DNA.

Xenopus egg extract preparation and assays

Demembranated sperm nuclei and interphase Xenopus egg extracts were prepared as described (Murray et al., 1991; Kubota and Takisawa, 1993). Further details are available in supplementary experimental procedures.

Generation of PrimPol knockout MEFS and metaphase chromosome preparations

The targeting of the PrimPol locus in mouse ES cells, generation of the PrimPol knockout mouse, and primary mouse fibroblasts lacking the PrimPol gene, are detailed in Figure S4. Mitotic MEF populations were enriched by colcemid (2×10^{-7}M) treatment for 1 to 2 hours, and following harvesting, were osmotically swollen, fixed, and placed on glass slides before staining with 5% Giemsa and microscopic analysis. See supplementary experimental procedures for further detail.

REFERENCES

Aguilera, A., & Gómez-González, B. (2008). Genome instability: a mechanistic view of its causes and consequences. Nat. Rev. Genet. *9*, 204-17.

Arlett, C. F., Harcourt, S. A., Broughton, B. C. (1975). The influence of caffeine on cell survival in excision-proficient and excision-deficient xeroderma pigmentosum and normal human cell strains following ultraviolet-light irradiation. *Mutation Res*. **33**, 341-6.

Bergoglio, V., Boyer, A. S., Walsh, E., Naim, V., Legube, G., Lee, M. Y., Rey, L., Rosselli, F., Cazaux, C., Eckert, K. A., & Hoffmann, J. S. (2013). DNA synthesis by Pol η promotes fragile site stability by preventing under-replicated DNA in mitosis. J. Cell Biol. *201*, 395-408.

Bétous, R., Pillaire, M. J., Pierini, L., van der Laan, S., Recolin, B., Ohl-Séguy, E., Guo, C., Niimi, N., Grúz, P., Nohmi, T., Friedberg, E., Cazaux, C., Maiorano, D., & Hoffmann, J. S. (2013). DNA polymerase κ-dependent DNA synthesis at stalled replication forks is important for CHK1 activation. EMBO J. *32*, 2172-85

Bocquier, A. A., Liu, L., Cann, I. K., Komori, K., Kohda, D., & Ishino, Y. (2001). Archaeal primase: bridging the gap between RNA and DNA polymerases. Curr. Biol. *11*, 452-6.

Bomgarden, R. D., Lupardus, P. J., Soni, D. V., Yee, M. C., Ford, J. M., & Cimprich, K. A. (2006). Opposing effects of the UV lesion repair protein XPA and UV bypass polymerase eta on ATR checkpoint signaling. *EMBO J*. *25*, 2605-14.

de Feraudy, S., Limoli, C. L., Giedzinski, E., Karentz, D., Marti, T. M., Feeney, L., & Cleaver, J. E. (2007). Pol η is required for DNA replication during nucleotide deprivation by hydroxyurea. Oncogene *26*, 5713-21.

Della, M., Palmbos, P. L., Tseng, H. M., Tonkin, L. M., Daley, J. M., Topper, L. M., Pitcher, R. S., Tomkinson, A. E., Wilson, T. E., & Doherty, A. J. (2004). Mycobacterial Ku and ligase proteins constitute a two-component NHEJ repair machine. Science *306*, 683-5.

Despras, E., Daboussi, F., Hyrien, O., Marheineke, K. & Kannouche, P. L. (2010). ATR/Chk1 pathway is essential for resumption of DNA synthesis and cell survival in UV- irradiated XP variant cells. Hum. Mol. Genet. *19*, 1690-701.

Edmunds, C. E., Simpson, L. J. & Sale, J. E. (2008). PCNA ubiquitination and REV1 define temporally distinct mechanisms for controlling translesion synthesis in the avian cell line DT40. Mol. Cell *30*, 519-29.

Elvers, I., Johansson, F., Groth, P., Erixon, K. & Helleday, T. (2011). UV stalled replication forks restart by re-priming in human fibroblasts. Nucleic Acids Res. *39*, 7049-57.

Frick, D. N., & Richardson, C. C. (2001). DNA primases. Annu. Rev. Biochem. *70*, 39-80.

Godoy, V. G., Jarosz, D. F., Walker, F. L., Simmons, L. A. & Walker, G. C. (2006). Y-family DNA polymerases respond to DNA damage-independent inhibition of replication fork progression. EMBO J. *25*, 868–79.

Heller, R. C., & Marians, K. J. (2006). Replication fork reactivation downstream of a blocked nascent leading strand. Nature *439*, 557-62.

Hirota, K., Sonoda, E., Kawamoto, T., Motegi, A., Masutani, C., Hanaoka, F., Szüts, D., Iwai, S., Sale, J. E., Lehmann, A. R., & Takeda, S. (2010). Simultaneous disruption of two DNA polymerases, Pol η and Pol ζ, in Avian DT40 cells unmasks the role of Pol η in cellular response to various DNA lesions. PLoS Genet. *6*, e1001151.

Iyer, L. M., Koonin, E. V., Leipe, D. D. & Aravind, L. (2005). Origin and evolution of the archaeo-eukaryotic primase superfamily and related palm-domain proteins: structural insights and new members. Nucleic Acids Res. *33*, 3875-96.

Johnson, R. E., Kondratick, C. M., Prakash, S. & Prakash, L. (1999). hRAD30 mutations in the variant form of xeroderma pigmentosum. Science *285*, 263–5.

Kannouche, P. L., Wing, J. & Lehmann, A. R. (2004). Interaction of human DNA polymerase η with monoubiquitinated PCNA: a possible mechanism for the polymerase switch in response to DNA damage. Mol Cell. *14*, 491-500.

Kubota, Y., & Takisawa, H. (1993). Determination of initiation of DNA replication before and after nuclear formation in Xenopus egg cell free extracts. J. Cell Biol. *123*, 1321-31.

Lehmann, A. R. (1972). Postreplication repair of DNA in ultraviolet-irradiated mammalian cells. J. Mol Biol. *66*, 319-37.

Li, X., & Heyer, W. D. (2008). Homologous recombination in DNA repair and DNA damage tolerance. Cell Res. *18*, 99–113.

Lipps, G., Röther, S., Hart, C., & Krauss, G. (2003). A novel type of replicative enzyme harbouring ATPase, primase and DNA polymerase activity. EMBO J. *22*, 2516– 25.

Lopes, M., Foiani, M., & Sogo, J. M. (2006). Multiple mechanisms control chromosome integrity after replication fork uncoupling and restart at irreparable UV lesions. Mol. Cell. *21*, 15-27.

Masutani, C., Kusumoto, R., Yamada, A., Dohmae, N., Yokoi, M., Yuasa, M., Araki, M., Iwai, S., Takio, K., & Hanaoka, F. (1999). The XPV (xeroderma pigmentosum variant) gene encodes human DNA polymerase η. Nature *399*, 700-4.

Michael, W. M., Ott, R., Fanning, E. & Newport, J. (2000). Activation of the DNA replication checkpoint through RNA synthesis by primase. Science *289*, 2133-7.

Murray, M. T., Krohne, G. & Franke, W. W. (1991). Different forms of soluble cytoplasmic mRNA binding proteins and particles in Xenopus laevis oocytes and embryos. J. Cell Biol. *112*, 1-11.

Narita, T., Tsurimoto, T., Yamamoto, J., Nishihara, K., Ogawa, K., Ohashi, E., Evans, T., Iwai, S., Takeda, S., & Hirota, K. (2010). Human replicative DNA polymerase δ can bypass T-T (6-4) ultraviolet photoproducts on template strands. Genes Cells. *15*, 1228-39.

O' Day, C. L., Burgers, P. M. & Taylor, J. S. (1992). PCNA-induced DNA synthesis past cis-syn and trans-syn-I thymine dimers by calf thymus DNA polymerase delta in vitro. Nucleic Acids Res. *20*, 5403-6.

Pagès, V. & Fuchs, R. P. (2003). Uncoupling of leading- and lagging-strand DNA replication during lesion bypass in vivo. Science *300*, 1300-3.

Pitcher, R. S., Brissett, N. C., & Doherty, A. J. (2007). Nonhomologous End-Joining in Bacteria: A Microbial Perspective. Annu. Rev. Microbiol. *61*, 259–82.

Sale, J. E., Lehmann, A. R., & Woodgate, R. (2012). Y-family DNA polymerases and their role in tolerance of cellular DNA damage. Nat. Rev. Mol. Cell Biol. *13*, 141-52.

Sonoda, E., Sasaki, M.S., Buerstedde, J.M., Bezzubova, O., Shinohara, A., Ogawa, H., Takata, M., Yamaguchi-Iwai, Y., and Takeda, S. (1998). Rad51-deficient vertebrate cells accumulate chromosomal breaks prior to cell death. EMBO J. *17*, 598-608.

Svoboda, D. L. & Vos, J. M. (1995). Differential replication of a single, UV-induced lesion in the leading or lagging strand by a human cell extract: fork uncoupling or gap formation. Proc. Natl. Acad. Sci. *92*, 11975-9.

Szuts, D., Marcus, A. P., Himoto, M., Iwai, S. & Sale, J. E. (2008). REV1 restrains DNA polymerase ζ to ensure frame fidelity during translesion synthesis of UV photoproducts in vivo. Nucleic Acids Res. *36*, 6767-80.

Van, C., Yan, S., Michael, W. M., Waga, S. & Cimprich, K. A. (2010). Continued primer synthesis at stalled replication forks contributes to checkpoint activation. J. Cell Biol. *189*, 233-46.

Yeeles, J. T. P., & Marians, K. J. (2011). The *Escherichia coli* replisome is inherently DNA damage tolerant. Science *334*, 235-8.

ACKNOWLEDGEMENTS

We declare that none of the authors have a financial interest related to this work. AJD laboratory was supported by a project grant from BBSRC and a centre grant from the MRC. HDL laboratory supported by North West Cancer Research Fund grants CR782 and CR869. THS laboratory was supported by a grant from the Ministerio de Ciencia e Innovación (SAF2009-10023), THS is a Ramon y Cajal fellow and IS is supported by a PhD studentship from Fundacio La Caixa. We thank Eva Petermann, Nadia Hégarat, Helfrid Hochegger, Alan Lehmann and Simone Sabbioneda for reagents, technical assistance and discussions. We also thank Shunichi Takeda for kindly providing Pol η DT40 cells and Shigenori Iwai who kindly provided DNA containing a 6-4 photoproduct.

FIGURE LEGENDS

Figure 1. Domain architecture and catalytic activities of human PrimPol

(**A**) Schematic and multiple sequence alignment of PrimPol conserved domains. The catalytic AEP domain containing three signature motifs (I, II and III) and the UL52-like zinc finger domain are indicated, including amino acid number. Multiple sequence alignment was generated with a selection of PrimPol homologues; blue shading indicates ≥40% sequence identity, red circles indicate residues required for metal ion binding, orange circle for nucleotide binding, and green circles for chelation of zinc.

(**B**) Primer synthesis by wild-type (WT) His-tagged human PrimPol and catalytic mutant (AxA). Homopolymer DNA templates (500 nM) were incubated with dNTPs or rNTPs (500 μM), magnesium ions, and WT or AxA PrimPol (1 μM) for 2 hours at 37^{o}C.

(**C**) DNA synthesis by PrimPol. Primer-template substrate (20 nM) and dNTPs (200 μM) were incubated with or without (−) PrimPol (WT or AxA; 50 nM) at 37^{o}C for increasing times (2, 5, 10, 15 minutes).

(**D**-**G**) DNA synthesis by PrimPol on templates containing either a T-T *cis-syn* cyclobutane pyrimidine dimer (CPD) (**D**), or a T-T pyrimidine (6-4) pyrimidone photoproduct (6-4 PP) (**E**-**G**), was compared to PrimPol DNA synthesis on undamaged templates using primer extension assays as described in (C). CPD is annealed opposite two 3' terminal dA residues thereby testing PrimPol extension opposite the lesion (D). 6-4 PP is at bases +1 and +2 of template relative to 3' terminus of primer to test read-through (E), and in the presence of single dNTPs for a single 30 minute reaction, to test nucleotide incorporation opposite 3' T (F, middle panel). Primer with 3' terminal dT opposite 3' T of 6-4 PP used to test nucleotide incorporation opposite 5' T of lesion (F, right panel) and, when all dNTPs included, extension (G). Note, undamaged template in (G) contains a 3' terminal T:T mismatch.

Figure 2. PrimPol is required for tolerance of UV photoproducts in a pathway independent of Pol η.

(**A**) Human (HEK-293) cells stably expressing PrimPol with a C-terminal Flag-Strep-II tag (PrimPol^{FlagStrep}) were either mock, UV-C (30 J/m^2), X-ray (5 Gy) irradiated, or treated for 6 hours with hydroxyurea (HU; 10 nM) and following recovery (1 hour for UV-C, 30 minutes for X-ray, immediately after HU treatment), were detergent extracted (0.5% Triton X-100) prior to

immunofluorecent (IF) analysis with an anti-PrimPol antibody and DAPI counterstaining.

(**B**) Representative images of nuclei containing detergent-resistant PrimPol foci.

(**C**) Proportion of cells in which PrimPol assembled into foci was determined at varying UV-C doses following an 8 hour recovery; error bars indicate SD of 3 experiments, >200 cells counted for each dose.

(**D**) Mock or UV-C irradiated (30 J/m^2) cells were allowed to recover for 8 hours before the Triton X-100 (0.5%) insoluble material was collected by centrifugation and treated with DNase and further centrifugated; the resulting samples were analyzed by Western blot with anti-PrimPol and PCNA antibodies.

(**E**) Normal human (MRC5) fibroblasts were either mock (−) or UV-C (30 J/m^2) irradiated, and following recovery, were separated into Triton X-100 (0.5%) soluble and insoluble material, and analyzed by Western blot along with whole cell extract (WCE).

(**F**) Normal (MRC5) fibroblasts or XP-V (XP30RO) patient cells were either mock or PrimPol siRNA treated and mock (−) or UV-C (2 J/m^2) irradiated and allowed to recover before cell lysates were prepared and analyzed by Western blot to determine levels of phosphorylated Chk1 on Ser345.

(**G**) UV-C clonogenic survival assays were performed with MRC5 and XP30RO cells either mock or PrimPol siRNA treated. Error bars denote SD of 3 experiments.

Figure 3. PrimPol is required for replication fork progression on UV damaged DNA templates in vertebrate cells.

(**A-C**) Viability of wild-type (WT) and DT40 knockout cell lines including PrimPol deficient cells expressing human PrimPol protein (PrimPol$^{-/-}$ +hPrimPol) was determined following exposure to UV-C (A), 4-nitroquinoline 1-oxide (4NQO; 48 hour treatment; B), and X-rays (C). Cells recovered for 48 hours after treatment before measuring metabolic capacity. Error bars denote SD of 3 experiments, with 2 PrimPol$^{-/-}$ cell lines used.

(**D**) Alkaline sucrose sedimentation analysis of DNA from cells that were either mock or UV-C irradiated (4 J/m^2) and immediately pulse-chased with ^{3}H-thymidine. Representative of at least 3 experiments shown; red arrow indicates post-replication repair defect.

(**E**) DNA fiber analysis of cells UV-C irradiated (20 J/m^2) between the CldU and IdU labeling periods. CldU:IdU ratio distribution representative of two sets of experiments using two PrimPol$^{-/-}$ cell lines (Cl1 and Cl2) is shown; >100 DNA fibers scored for each. The average of this data is presented as a cumulative percentage of forks at each ratio (**F**). See Figure S3 for details on the knockout cells.

Figure 4. PrimPol functions during an unperturbed S-phase.

(**A**) His-tagged PrimPol (PrimPol at 12 ng/µl) was added to *Xenopus* egg extract supplemented with sperm nuclei. Extracts were treated with geminin (80 nM), roscovitine (0.5 mM) or aphidicolin (100 µg/ml) and incubated at 21°C. At the indicated times (minutes), chromatin was isolated and associated proteins subjected to Western blot analysis with the antibodies indicated. (**B**) Experiment in **A** was repeated at a 60 minute time point and the last lane corresponds to a sample pre-incubated with geminin followed by aphidicolin treatment.

(**C**) Analysis of metaphase aberrations in mock and aphidicolin treated primary MEFs lacking PrimPol. Percentage and type of aberrations per chromosome are indicated. Examples of two chromatid breaks and two rearrangements from PrimPol deficient cells are shown. See Figure S4 for details on the knockout cells.

(**D**) Model of PrimPol-mediated replication fork progression. Following DNA replication stalling (depicted on the leading strand) PrimPol could re-prime DNA synthesis downstream of the lesion to allow DNA replication to continue. PrimPol can also catalyse TLS of some DNA lesions and could directly extend the stalled primer terminus facilitating replication fork progression. With regards to UV-damaged templates, PrimPol could function in the error-free extension from CPDs and the error-prone bypass of 6-4 PPs.

SUPPLEMENTAL INFORMATION

Supplementary information including four results figures, experimental procedures and three tables can be found at…

Figure 1

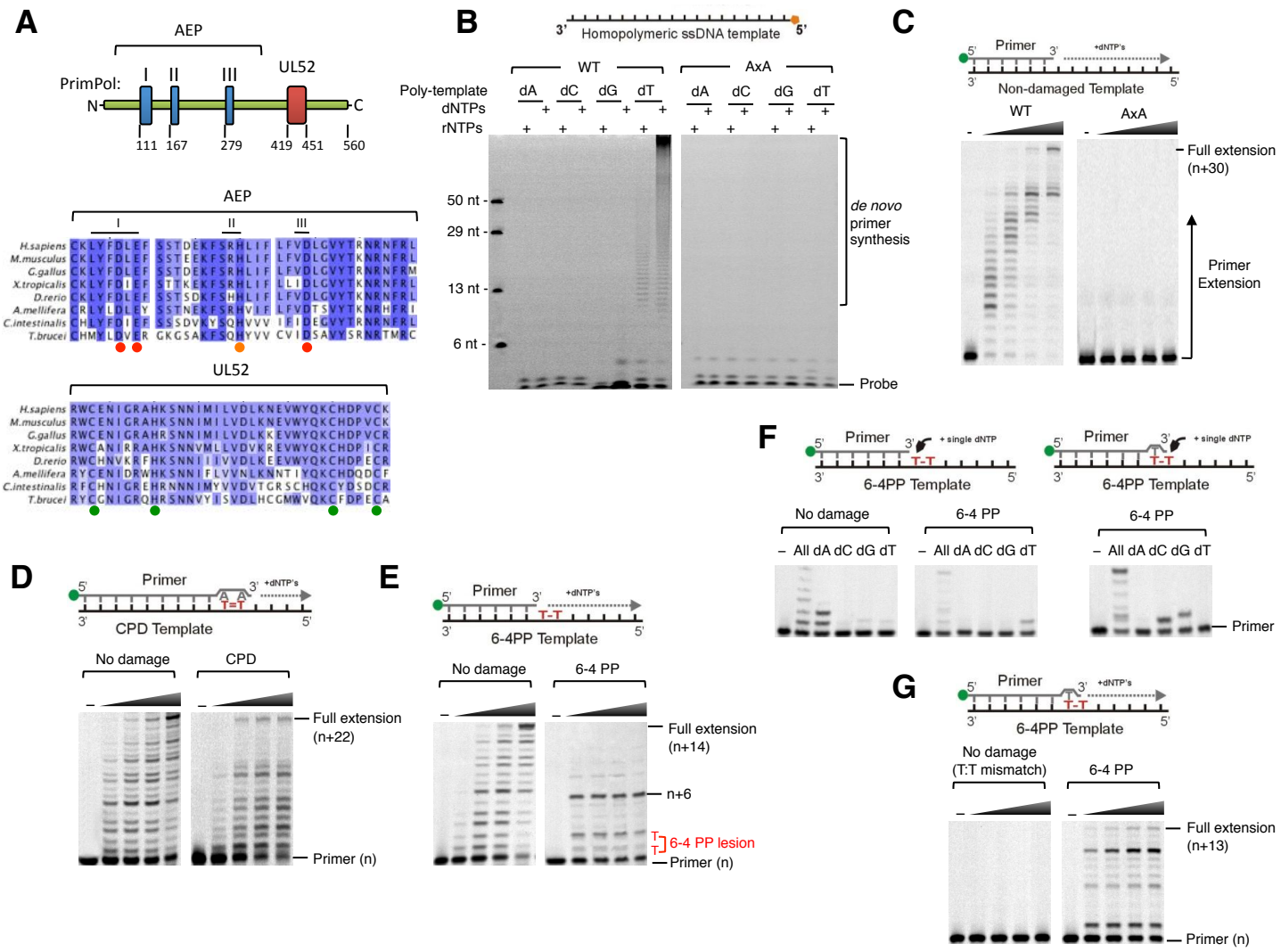

Figure 1

Figure 2

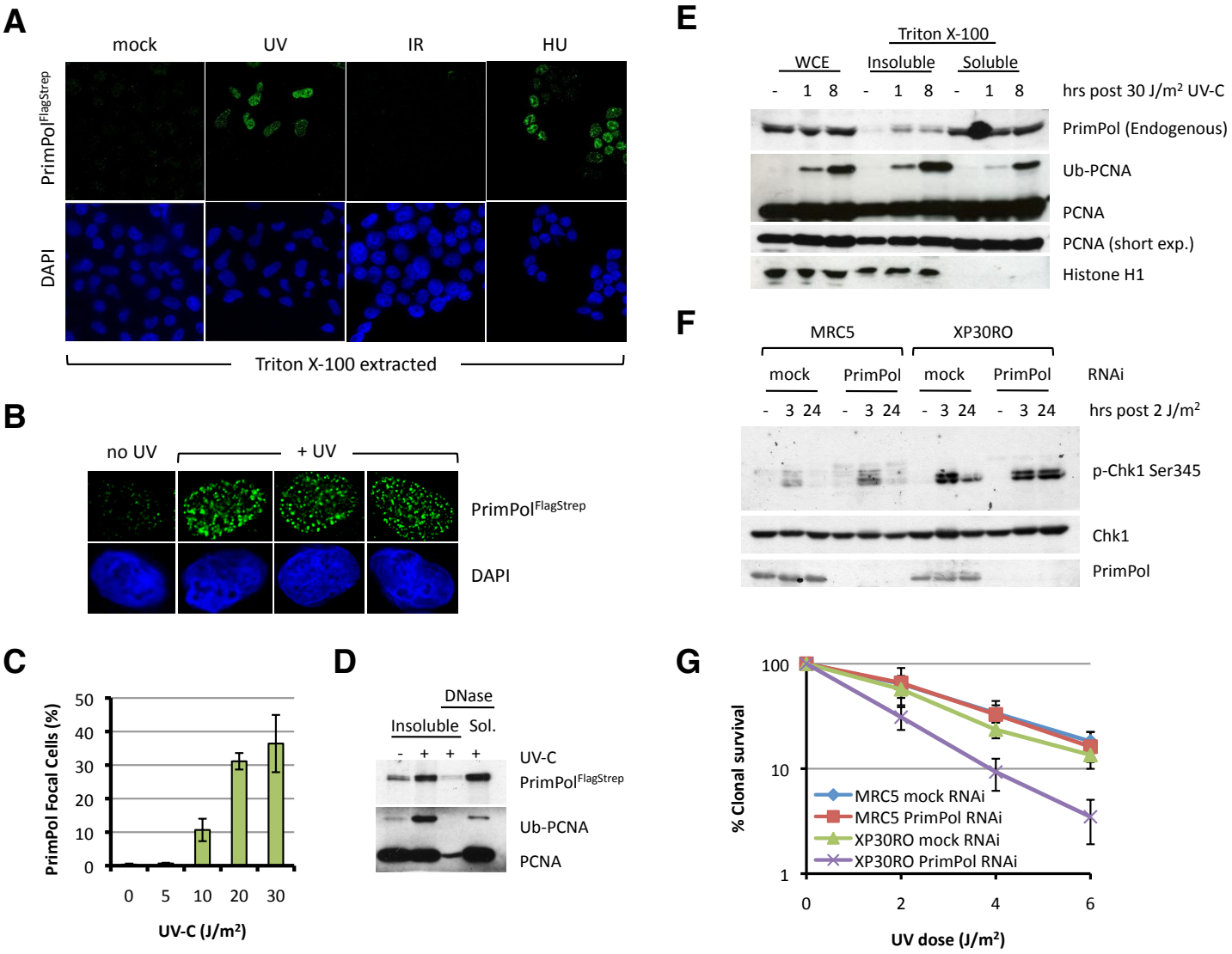

Figure 2

Figure 3

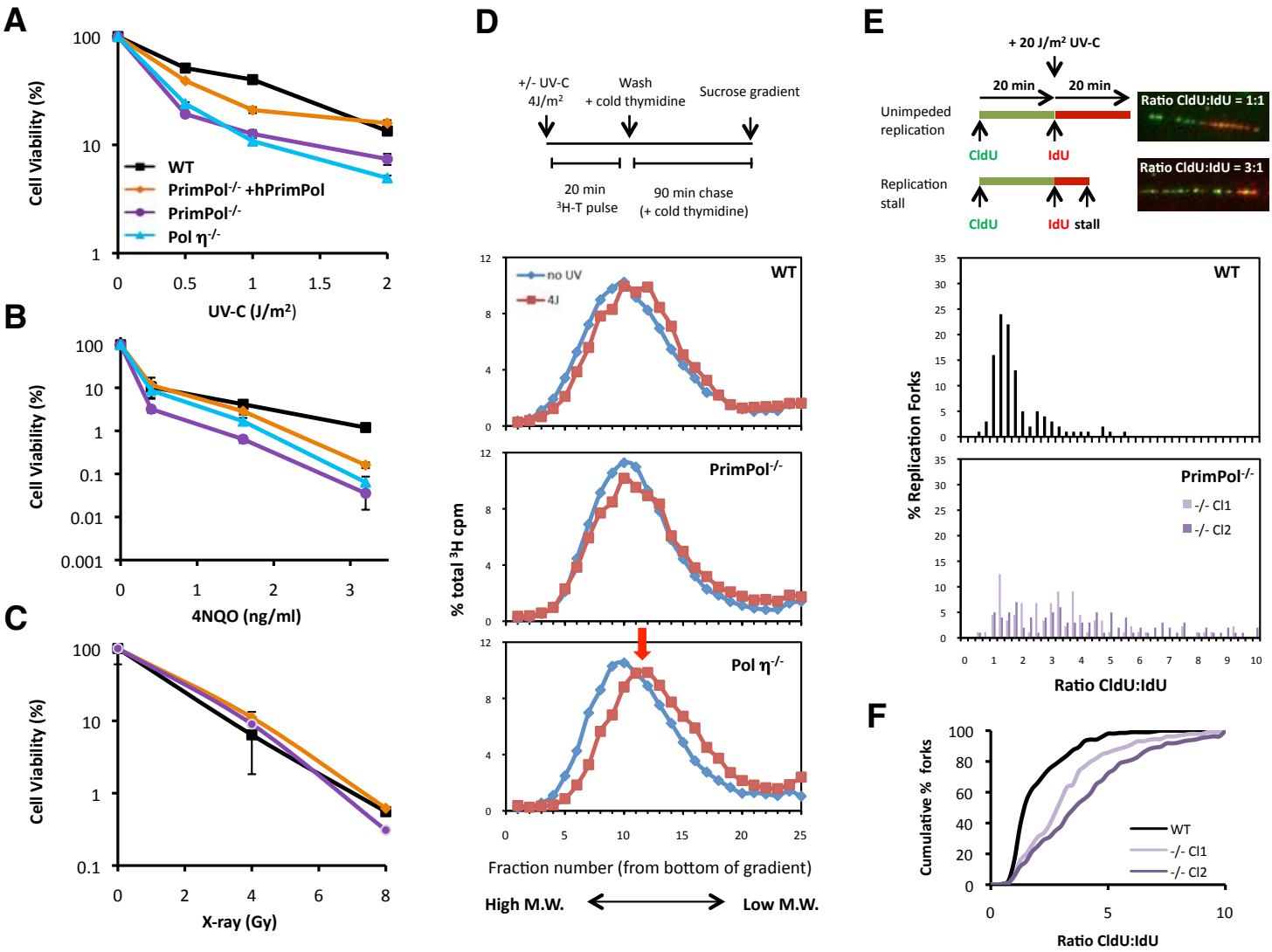

Figure 3

Figure 4

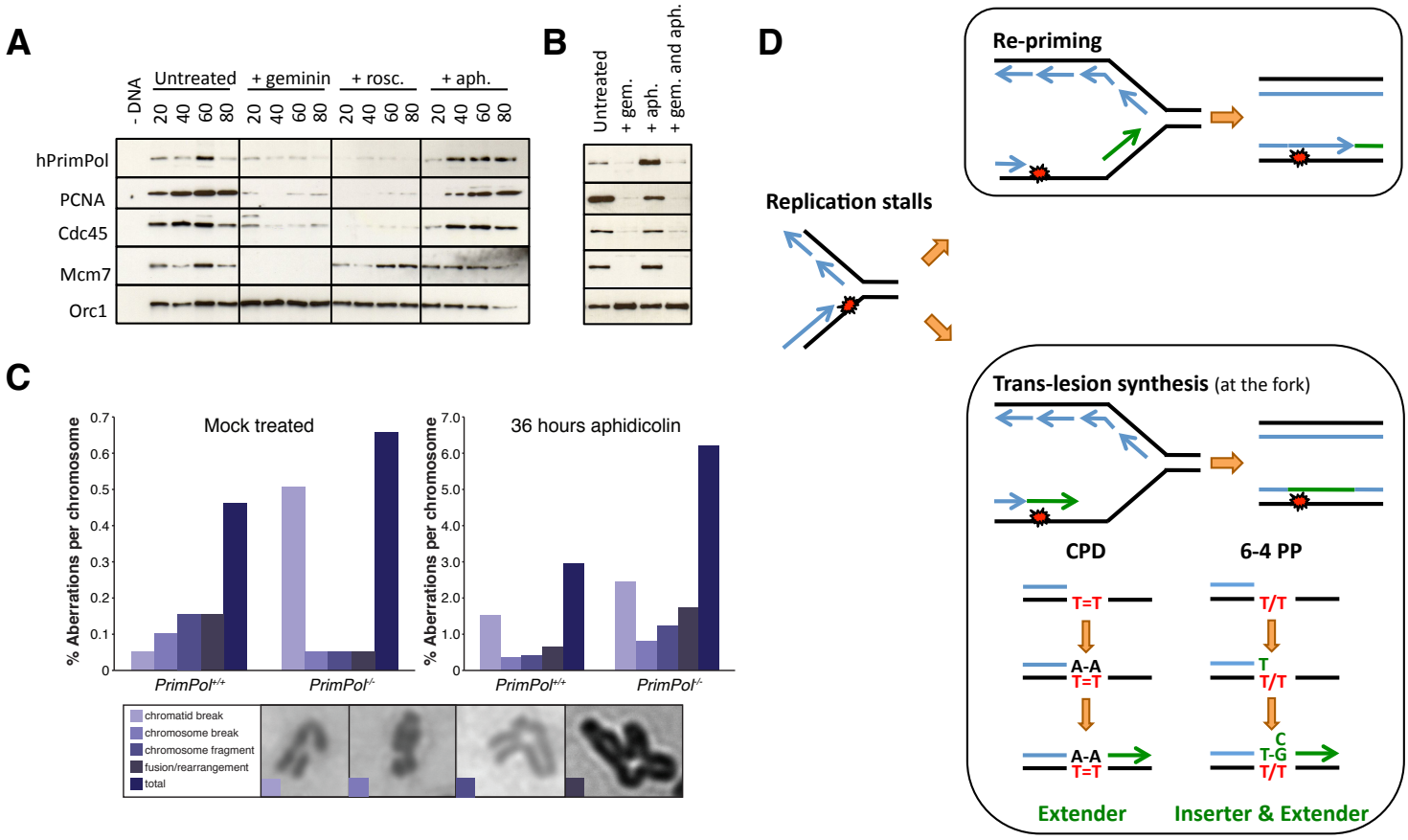

Figure 4

SUPPLEMENTARY INFORMATION INVENTORY

Four supplementary results figures

Figure S1. Primer extension assays with human PrimPol, human Pol ε, and archaeal replicase Tgo-Pol.

This figure is related to Figure 1 and presents the purification gels of WT and AxA PrimPol recombinant proteins, supplementary primer extensions with damaged DNA templates, and extension assays performed on control DNA substrates or with control DNA polymerases (Pol ε and Tgo-Pol).

Figure S2. PrimPol sub-cellular localisation and RNAi phenotype analysis in cultured human cells.

This figure is related to Figure 2 and details the generation of human stable cell lines and IF detection of endogenous and over-expressed PrimPol. Phenotypic analysis of PrimPol RNAi treated cells is also included, analysing RPA and Rad51 foci formation and clonogenic survival experiments performed in XP-V or XPA cell lines.

Figure S3. Generation and characterisation of PrimPol knockout DT40 cell lines.

This figure is related to Figure 3 and explains the generation of DT40 knockout cell lines and their preliminary characterisation during unperturbed conditions or following UV-C irradiation.

Supplementary Figure S4. PrimPol chromatin-association following aphidicolin treatment and generation of PrimPol knockout MEFs.

This figure is related to Figure 4 and shows human PrimPol chromatin-association after aphidicolin treatment, and explains the generation of PrimPol knockout mice.

Three supplementary tables

Table S1. Primer-template substrates.

This table is related to the Experimental Procedures and details the sequence of the oligoucleotides used in the primer-extension assays.

Table S2. DT40 PrimPol knockout primers.

This table is related to the Experimental Procedures and details the sequence of the primers used to target PrimPol gene in DT40 cells.

Table S3. Southern blot probe and RT-PCR primers.

This table is related to the Experimental Procedures and details the sequence of the primers used to screen and confirm the PrimPol knockout in DT40 cells.

Supplemental experimental procedures and references

Detailed experimental procedures are included.

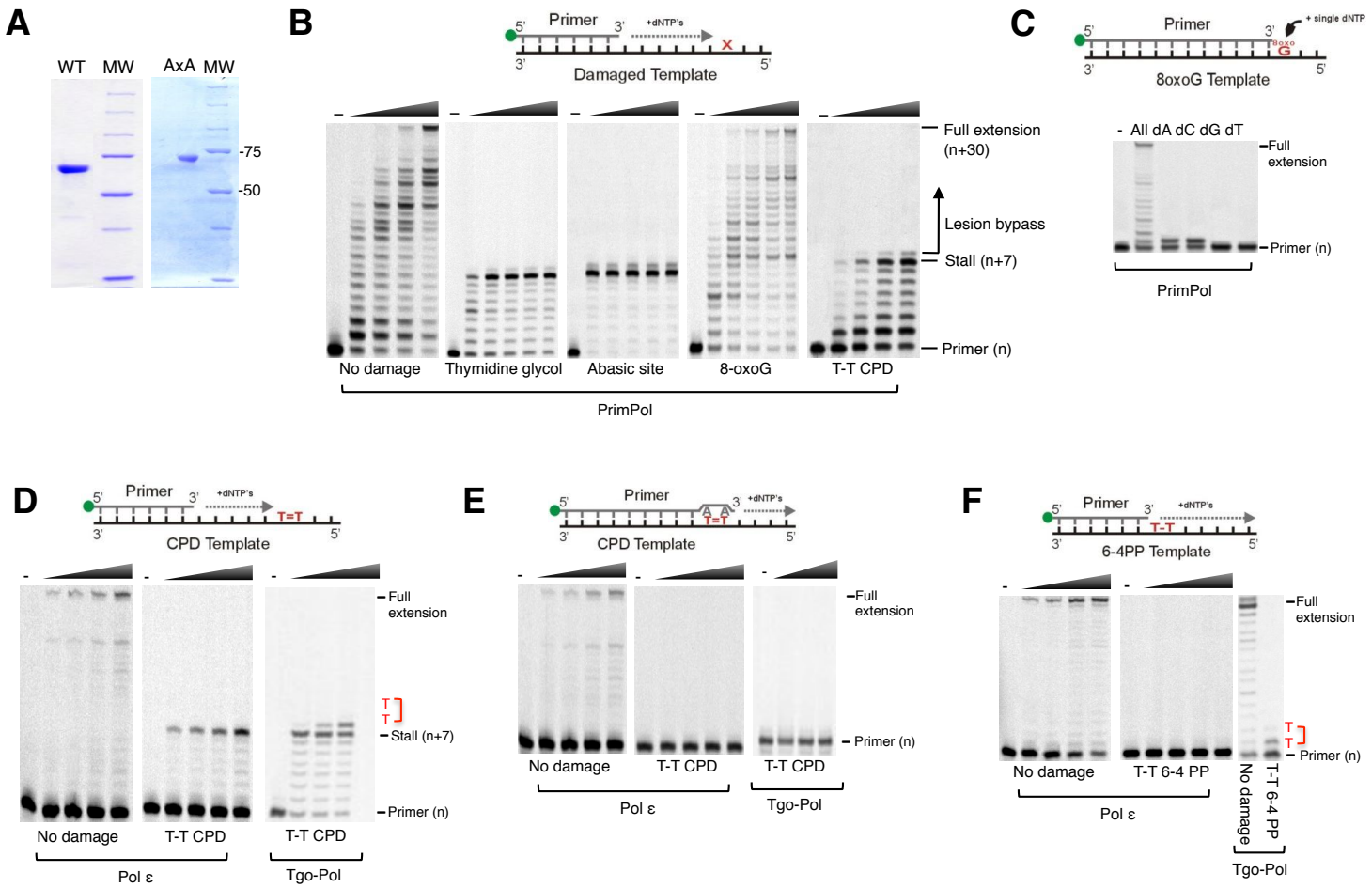
A
WT
MW
AxA
MW
-75
-50
B
Primer
+dNTP's
Damaged Template
Full extension (n+30)
Lesion bypass
Stall (n+7)
Primer (n)
No damage
Thymidine glycol
Abasic site
8-oxoG
T-T CPD
PrimPol
C
Primer
+ single dNTP
8oxoG Template
- All dA dC dG dT
Full extension
Primer (n)
PrimPol
D
Primer
+dNTP's
CPD Template
Full extension
Stall (n+7)
Primer (n)
No damage
T-T CPD
T-T CPD
Pol ε
Tgo-Pol
E
Primer
+dNTP's
CPD Template
Full extension
Primer (n)
No damage
T-T CPD
T-T CPD
Pol ε
Tgo-Pol
F
Primer
+dNTP's
6-4PP Template
Full extension
Primer (n)
No damage
T-T 6-4 PP
Pol ε
No damage
T-T 6-4 PP
Tgo-Pol

Figure S1

Figure S1. Primer extension assays with human PrimPol, human Pol ε, and archaeal replicase Tgo-Pol (linked to Figure 1)

(**A**) SDS PAGE analysis of wild-type (WT) His-tagged human PrimPol and catalytic mutant (AxA).

(**B**) DNA synthesis by PrimPol on DNA templates containing a thymidine glycol lesion, abasic site, 8-oxo-Guanine (8-oxoG), or T-T *cys-sin* cyclobutane pyrimidine dimer (CPD), was compared to DNA synthesis on an undamaged template using primer extension assays. Primer-template substrate (20 nM) and dNTPs (200 μM) were incubated with or without (–) WT PrimPol (50 nM) at 37^{o}C for increasing times (2, 5, 10, 15 minutes, indicated by the black triangle). Thymidine glycol, abasic site, and 8-oxoG were positioned at bases +8 of the template relative to 3' terminus of primer, whilst the CPD was positioned at bases +8 and +9, to test read-through by PrimPol.

(**C**) DNA synthesis by PrimPol on a DNA template containing an 8-oxoG lesion. Primer extension performed as in (B) except individual dNTPs were added for a single 30 minute time point. 8-oxoG is at base +1 of the template relative to the 3' terminus of the primer to test single nucleotide incorporation opposite the lesion.

(**D** – **F**) DNA synthesis by human Pol ε and archaeal replicase from *Thermococcus gorgonarius* (Tgo-Pol exo-) on DNA templates containing a T-T CPD (**D** and **E**) or a T-T pyrimidine (6-4) pyrimidone photoproduct (6-4 PP) (**F**) was compared to DNA synthesis on undamaged templates using primer extension assays. Human Pol ε (100 nM) was incubated with the indicated primer-template substrate (20 nM) and dNTPs (200 μM) in reaction buffer for increasing times (2, 5, 10, 20 minutes, indicated by black triangle) at 37^{o}C. For Tgo-Pol reactions, 50 nM enzyme was used and the reaction incubated for a single 30 minutes time point or increasing times (30, 60, 120 seconds, black triangle). No enzyme controls (–) were performed in similar conditions. CPD is at bases +8 and +9 of template relative to 3' terminus of primer to test read-through (D), or annealed opposite two 3' terminal dA residues thereby testing polymerase extension opposite the lesion (E). 6-4 PP is at bases +1 and +2 of template relative to 3' terminus of primer to test read-through (F).

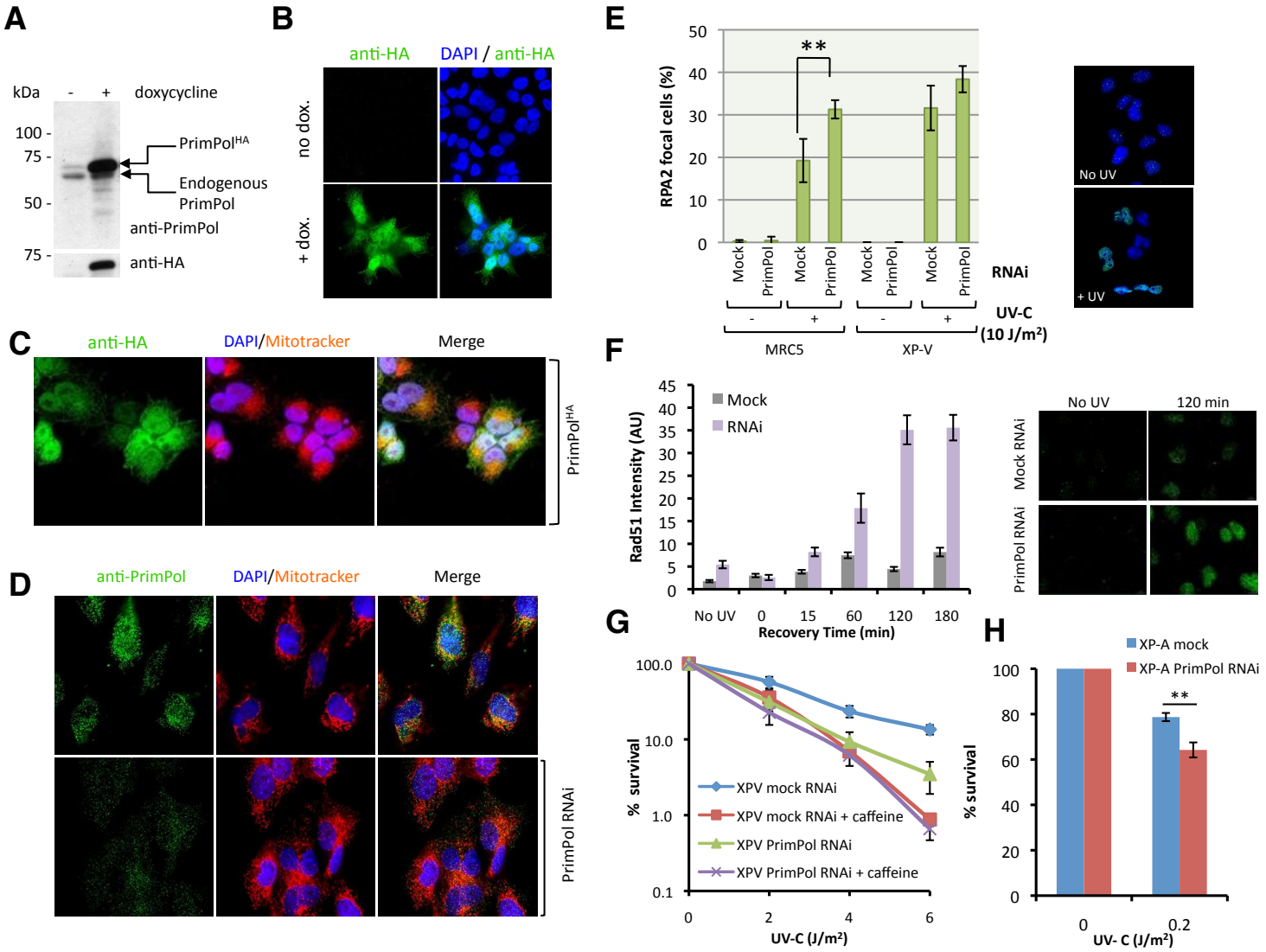
A
kDa
-
+
doxycycline
100 -
75 -
50 -
75 -
PrimPol^HA
Endogenous PrimPol
anti-PrimPol
anti-HA
B
anti-HA
DAPI / anti-HA
no dox.
+ dox.
C
anti-HA
DAPI/Mitotracker
Merge
PrimPol^HA
D
anti-PrimPol
DAPI/Mitotracker
Merge
PrimPol RNAi
E
RPA2 focal cells (%)
50
40
30
20
10
0
**
Mock
PrimPol
Mock
PrimPol
Mock
PrimPol
Mock
PrimPol
RNAi
UV-C (10 J/m²)
-
+
-
+
MRC5
XP-V
No UV
+ UV
F
Rad51 Intensity (AU)
45
40
35
30
25
20
15
10
5
0
Mock
RNAi
No UV
0
15
60
120
180
Recovery Time (min)
No UV
120 min
Mock RNAi
PrimPol RNAi
G
% survival
100.0
10.0
1.0
0.1
XPV mock RNAi
XPV mock RNAi + caffeine
XPV PrimPol RNAi
XPV PrimPol RNAi + caffeine
0
2
4
6
UV-C (J/m²)
H
XP-A mock
XP-A PrimPol RNAi
% survival
100
80
60
40
20
0
**
0
0.2
UV- C (J/m²)

Figure S2

Figure S2. PrimPol sub-cellular localisation and RNAi phenotype analysis in cultured human cells (linked to Figure 2)

(**A** - **C**) Flp-In T-REx-293 cells engineered for inducible expression of recombinant PrimPol fused to a C-terminal HA epitope ($PrimPol^{HA}$) were grown in the absence or presence of 10 ng/ml doxycycline for 18 hours before analysis. Cell lysates were prepared and analysed by Western blot with an anti-PrimPol and an anti-HA antibody (A). Fixed cells were subjected to immunofluorescent analysis with an anti-HA antibody (green) and DAPI counterstaining (blue) (B). Prior to fixing and immunofluorescent staining with anti-PrimPol (green) and counterstainig with DAPI (blue), cells were incubated with Mitotracker Deep Red (red) to stain mitochondria (C).

(**D**) Immunofluorescent detection of endogenous PrimPol. 143B cells were either mock or PrimPol RNAi treated and 48 hours after, subjected to immunofluorescent analysis with an anti-PrimPol antibody (green). Cells were counterstained with Mitotracker Deep Red to visualize mitochondria (red) and DAPI to visualize nuclei (blue).

(**E**) Normal (MRC5) and XP-V (XP30RO) fibroblasts were either mock or PrimPol RNAi treated and at 72 hours seeded on glass coverslips. The next day cells were either mock or UV-C (10 J/m^2) irradiated and following a 6 hour recovery, were Triton X-100 (0.5%) extracted and subjected to immunofluorescent analysis with anti-RPA2 and DAPI counterstaining. The proportion of cells with focal RPA2 (> 20 foci per nuclei) were determined, at least 200 cells were counted from each sample, error bars denote SD of 3 experiments. Significance was determined with the two-tailed T-test (**< 0.01). Representative images are shown on the right panel.

(**F**) XP-V cells were either mock or PrimPol RNAi treated then either mock or UV-C (3 J/m^2) irradiated; following different recovery times, cells were Triton X-100 (0.1%) extracted and subjected to immunofluorescent analysis with Rad51 antibody and DAPI counterstaining. Intensity of the signal was measured by Image J, error bars denote SD of 2 experiments. Representative images are shown on the right panel.

(**G**) XP-V cells were mock or PrimPol RNAi treated. At 24 hours they were seeded on 9cm dishes in duplicate and allowed to attach. Cells were then treated with 0-6 J/m^2 UV-C with or without the addition of 0.38 mM caffeine. Colonies were allowed to form over 10 days when cells were fixed and stained with methylene blue. Error bars show SD of 3 experiments.

(**H**) Role of PrimPol in NER. XP-A cells were mock or PrimPol RNAi treated. Following RNAi cells were seeded to replicate 9cm plates and allowed to attach. Cells were then treated with 0 or 0.2 J/m^2 UV-C and

colonies were allowed to form over approximately 10 days. Colonies were stained with methylene blue and counted to compare survival. Error bars represent SD of the mean of 3 experiments, significance was determined using the T-test ($p = 0.006$).

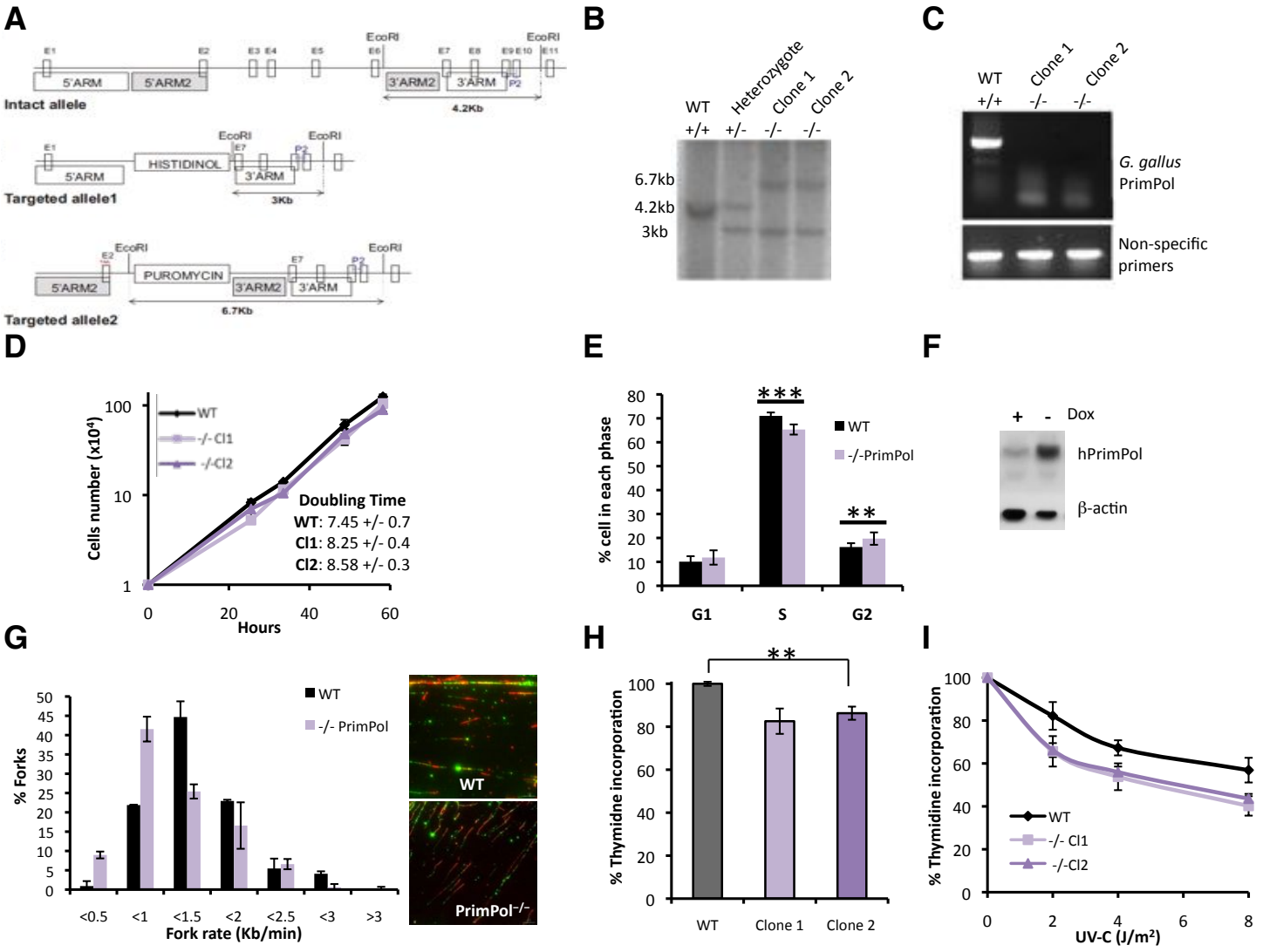
A
Intact allele
5'ARM
5'ARM2
3'ARM2
3'ARM
4.2Kb
Targeted allele1
HISTIDINOL
3Kb
Targeted allele2
PUROMYCIN
6.7Kb
B
WT
Heterozygote
Clone 1
Clone 2
+/+
+/-
-/-
6.7kb
4.2kb
3kb
C
G. gallus PrimPol
Non-specific primers
D
Cells number (x10⁴)
Hours
WT
-/- Cl1
-/-Cl2
Doubling Time
WT: 7.45 +/- 0.7
Cl1: 8.25 +/- 0.4
Cl2: 8.58 +/- 0.3
E
% cell in each phase
G1
S
G2
WT
-/-PrimPol
F
Dox
hPrimPol
β-actin
G
% Forks
Fork rate (Kb/min)
-/- PrimPol
PrimPol-/-
H
% Thymidine incorporation
I
UV-C (J/m²)

Figure S3

Figure S3. Generation and characterisation of PrimPol knockout DT40 cell lines (linked to Figure 3)

(**A**) Illustration of Southern blot strategy used to disrupt *G. gallus PrimPol* gene; exons (square boxes), EcoRI restriction sites and Southern blot probe (P2) are depicted along with expecting band size (under horizontal arrows) for Southern blot analysis. Both disruption cassettes (histidinol and puromycin) are flanked by two distinct sets of recombination arms (white or grey boxes) in order to specifically target the wild-type allele remaining in heterozygote clones WT/HIS.

(**B**) Southern blot of genomic DNA of WT DT40 cells (+/+) and clones obtained after *PrimPol G. gallus* gene disruption showing the loss of both wild-type alleles in clone 1 and 2 (–/–) or only one allele remaining in the heterozygote clone (+/–).

(**C**) RT-PCR performed on RNA extracted from WT and both KO clones, using *G. gallus PrimPol* specific primers (upper gel) or unspecific *G. gallus* primers (lower gel) as PCR control.

(**D**) Growth curves of WT (black line) and PrimPol$^{-/-}$ (light and dark purple) DT40 cells were assessed by counting duplicate cultures of each population over 7 generations (56 hours), using a haemocytometer with trypan blue dye exclusion staining. Doubling time for each population was determined using an exponential regression algorithm; average and SD were calculated from 3 independent experiments.

(**E**) Cell cycle profile of WT DT40 (black) or average of both PrimPol$^{-/-}$ clones (purple) was determined using flow cytometry after BrdU incorporation. Error bars denote SD of 5 experiments, and significance was determined with the two-tailed T-test (***<0.001, **<0.01).

(**F**) Western blot analysis of PrimPol$^{-/-}$ clone expressing human PrimPol under a tetracycline (tet off) promoter; doxycycline was added at 1 mg/ml for 24 hours; anti-PrimPol and anti beta-actin antibodies were used.

(**G**) Distribution of replication fork speeds in unperturbed wild-type (WT) and PrimPol$^{-/-}$ DT40 cells was determined by DNA fiber analysis. Error bars denote SD of 2 experiments with > 100 DNA fibers analyzed each time, with two PrimPol$^{-/-}$ cell lines used.

(**H**) WT (black line) and both PrimPol$^{-/-}$ (light and dark purple lines) DT40 cells were pulse-labeled for 20 minutes with ^{3}H-thymidine following UV-C irradiation. Incorporation rate was calculated and normalised against undamaged cells using ^{14}C-thymidine overnight pre-labeling for total DNA normalisation. Error bars represent SD of 3 independent experiments.

(**I**) WT (grey) and PrimPol$^{-/-}$ (light and dark purple) DT40 cells were first labeled with ^{14}C-thymidine for 16 hours and then pulse-labeled for 20 minutes with ^{3}H-thymidine. Incorporation rate was calculated after normalisation with ^{14}C signal for total DNA content. Error bars represent SD of 3 independent experiments.

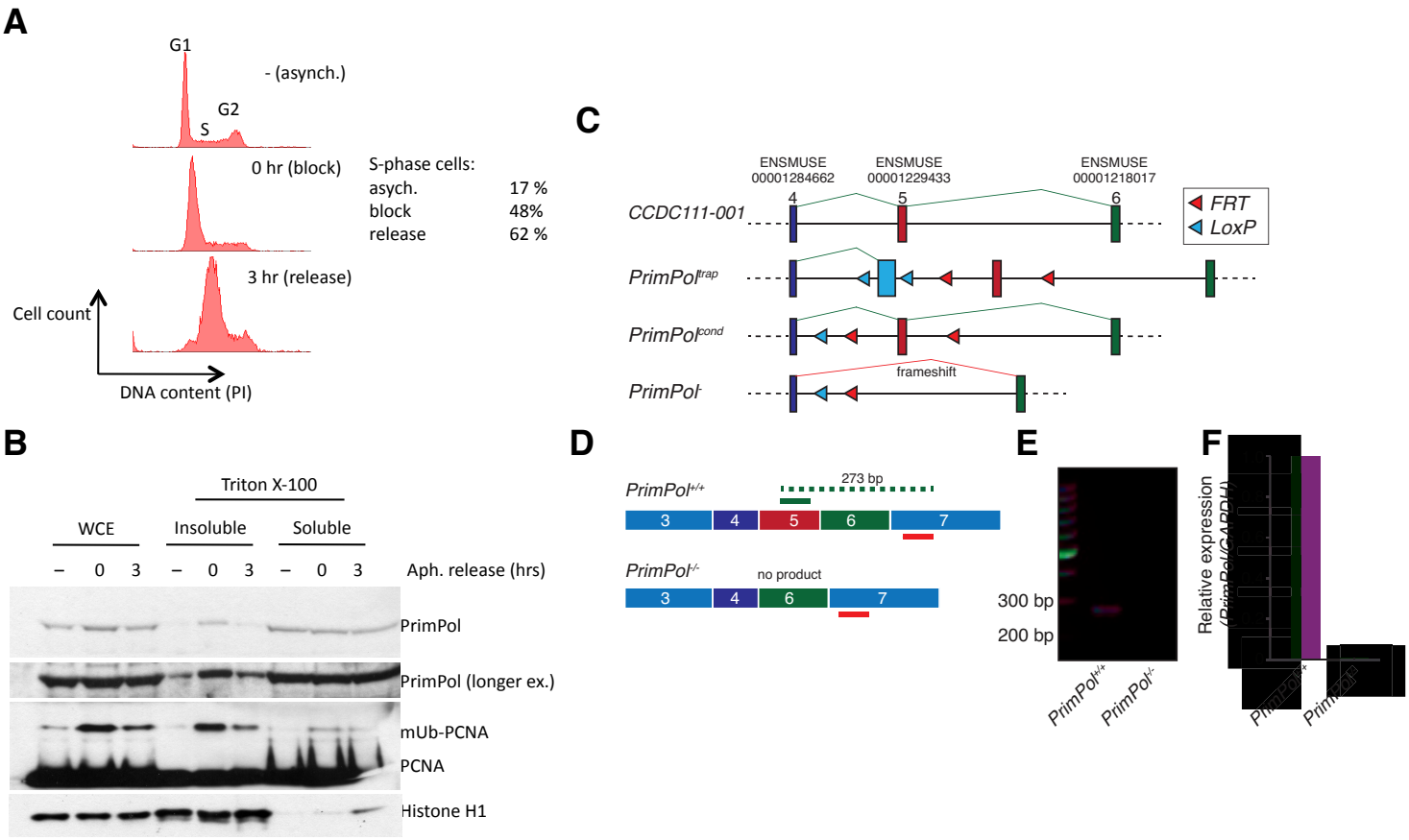
A
G1
- (asynch.)
G2
S
0 hr (block)
3 hr (release)
Cell count
DNA content (PI)
S-phase cells:
asych. 17 %
block 48%
release 62 %
B
Triton X-100
WCE
Insoluble
Soluble
– 0 3 – 0 3 – 0 3
Aph. release (hrs)
PrimPol
PrimPol (longer ex.)
mUb-PCNA
PCNA
Histone H1
C
ENSMUSE 00001284662
ENSMUSE 00001229433
ENSMUSE 00001218017
4
5
6
CCDC111-001
PrimPol^trap
PrimPol^cond
PrimPol-
frameshift
FRT
LoxP
D
PrimPol+/+
273 bp
3 4 5 6 7
PrimPol-/-
no product
3 4 6 7
E
300 bp
200 bp
PrimPol+/+
PrimPol-/-
F
Relative expression
(PrimPol/GAPDH)

Figure S4

Figure S4. PrimPol chromatin-association following aphidicolin treatment and generation of PrimPol knockout MEFs (linked to Figure 4)

(**A**) SV40-transformed normal (MRC5) fibroblasts were grown in the presence or absence of 2 μg/ml aphidicolin for 16 hours, and then the aphidicolin was removed and cells allowed to grow for a further 3 hours before analysis. Cells were fixed, stained with PI, and analysed by flow cytometry to determine the DNA content and the proportion of S-phase cells.

(**B**) PrimPol becomes insoluble following prolonged aphidicolin treatment, suggesting chromatin binding. MRC5 fibroblasts were either mock (-) or aphidicolin treated (2 μg/ml, ~16 hours) and allowed to recover for the time indicated before being separated into Triton X-100 soluble and insoluble fractions and subjected to Western blot analysis with antibodies indicated. Histone H1 was used to detect chromatin, PCNA and the slower migrating mono-ubiquitylated (Ub)-PCNA indicates stalled replication forks.

(**C**) Schematic of modified murine PrimPol locus (CCDC111). Dark blue and green boxes represent exons, red box the targeted exon 5 (contains the entire AEP I signature motif), light blue box the genetrap cassette, light blue triangles FRT sites, red triangles LoxP sites and green lines predicted splicing patterns confirmed by analysis of cDNA.

(**D**) Real time PCR strategy for the assessment of relative mRNA levels in MEFs.

(**E**) Agarose gel electrophoresis of PCR products from PrimPol primers and cDNA of the indicate genotype.

(**F**) Real time PCR analysis of PrimPol mRNA levels in wild type and PrimPol-/- animals.

Table S1. Primer-template substrates (related to Experimental Procedures)

Figure	Primer (5'→3')	Template (5'→3')
1C	TGTCGTCTGTTCGGTCGTTC	CGCGCAGGGCGCACAACAGCCTTGAAGACCGAACGACCGAACAGACGACA
1D	TGTCGTCTGTTCGGTCGTTCGGTCTTCAA	CGCGCAGGGCGCACAACAGCCTTGAAGACCGAACGACCGAACAGACGACA or CGCGCAGGGCGCACAACAGCC(T=T)GAAGACCGAACGACCGAACAGACGACA
1E	CACTGACTGTATGATG	CTCGTCAGCATCTTCATCATACAGTCAGTG or CTCGTCAGCATC(T/T)CATCATACAGTCAGTG
1F	CACTGACTGTATGATG	CTCGTCAGCATCTTCATCATACAGTCAGTG or CTCGTCAGCATC(T/T)CATCATACAGTCAGTG
1F	CACTGACTGTATGATGT	CTCGTCAGCATC(T/T)CATCATACAGTCAGTG
1G	CACTGACTGTATGATGT	CTCGTCAGCATCTTCATCATACAGTCAGTG or CTCGTCAGCATC(T/T)CATCATACAGTCAGTG
S1B	TGTCGTCTGTTCGGTCGTTC	CGCGCAGGGCGCACAACAGCCTTGAAGACCGAACGACCGAACAGACGACA or CGCGCAGGGCGCACAACAGCC(Tg)TGAAGACCGAACGACCGAACAGACGACA or CGCGCAGGGCGCACAACAGCC(AP)TGAAGACCGAACGACCGAACAGACGACA or CGCGCAGGGCGCACAACAGCC(oxoG)TGAAGACCGAACGACCGAACAGACGACA or CGCGCAGGGCGCACAACAGCC(T=T)GAAGACCGAACGACCGAACAGACGACA
S1C	TGTCGTCTGTTCGGTCGTTCGGTCTTCA	CGCGCAGGGCGCACAACAGCC(oxoG)TGAAGACCGAACGACCGAACAGACGACA
S1D	TGTCGTCTGTTCGGTCGTTC	CGCGCAGGGCGCACAACAGCCTTGAAGACCGAACGACCGAACAGACGACA or CGCGCAGGGCGCACAACAGCC(T=T)GAAGACCGAACGACCGAACAGACGACA
S1E	TGTCGTCTGTTCGGTCGTTCGGTCTTCAA	CGCGCAGGGCGCACAACAGCCTTGAAGACCGAACGACCGAACAGACGACA or CGCGCAGGGCGCACAACAGCC(T=T)GAAGACCGAACGACCGAACAGACGACA
S1F	CACTGACTGTATGATG	CTCGTCAGCATCTTCATCATACAGTCAGTG or CTCGTCAGCATC(T/T)CATCATACAGTCAGTG

DNA lesions are indicated in red text: T=T, thymine-thymine *cys-sin* cyclobutane pyrimidine dimer (T-T CPD); T/T, thymine-thymine pyrimidine 6-4 pyrimidone photoproduct (T-T 6-4 PP); Tg, thymidine glycol; AP, abasic site; oxoG, 8-oxo-Guanine.

Table S2. DT40 PrimPol knockout primers (linked to Experimental Procedures)

Histidinol upstream ARM primer FOR	5′-GGGGACAACTTTGTATAGAAAAGTTGGGCGGCAGCGCGCGGGCCGCGGAGAGG-3′
Histidinol upstream ARM primer REV	5′-GGGGACTGCTTTTTTGTACAAACTTGTATACATTTAAATATCTTTGTGGATC-3′
Histidinol downstream ARM primer FOR	5′-GGGGACAGCTTTCTTGTACAAAGTGGTGAGAGGGGAGCTGAAAGCAGTTT-3′
Histidinol downstream ARM primer REV	5′-GGGGACAACTTTGTATAATAAAGTTGCCATGGGCTCTGTTTAAACAAACAAGC-3′
Puromycin upstream ARM primer FOR	5′-GGGGACAACTTTGTATAGAAAAGTTGTTAAAGGTTTGAGTGATTCTGAATATAGCC-3′
Puromycin upstream ARM primer REV	5′-GGGGACTGCTTTTTTGTACAAACTTGTTACTCCTTGCAGGTTTTCACAAATC-3′
Puromycin downstream ARM primer FOR	5′-GGGGACAGCTTTCTTGTACAAAGTGGAACCAAATACAGTCCATGCTGAAAC-3′
Puromycin downstream ARM primer REV	5′-GGGGACAACTTTGTATAATAAAGTTGGTGGCCAACTAAGACTATGCAAAC-3′

Table S3. Southern blot probe and RT-PCR primers (linked to Experimental Procedures)

Southern blot probe, primer FOR	5′-ACGGAGTGCAAGGAGGTAAC-3′
Southern blot probe, primer REV	5′-GACTGGATCGTGGCACTTC-3′
G. gallus PrimPol cDNA, primer FOR	5′-ATGAAGAGAAAATGGGAAGAAAGAGTGAAGAAAGTTG -3′
G. gallus PrimPol cDNA, primer REV	5′-AGCCTTTGGAAGCATCTTCGACT-3′
G.gallus Bora cDNA, primer FOR	5′- ATGGGCGATACAGAAGAAGCCCAAATGCAG-3′
G.gallus Bora cDNA, primer REV	5′-CTCGAGAGGAGAAGGAACTATGAGACTCTTTGTGAAAACTCC-3′

SUPPLEMENTARY EXPERIMENTAL PROCEDURES

Purification of recombinant proteins

Human PrimPol cDNA was sub-cloned into pET28a (Novagen) using NdeI and BamHI restriction sites to generate a 6-histidine N-terminal tagged recombinant protein. Catalytic null mutant AxA (D114A and E116A) was obtained by site directed mutagenesis PCR of this construct using forward 5'-AGCTTTATTTTGCTTTGGCATTTAACAAACC-3' and reverse 5'-GGTTTGTTAAATGCCAAAGCAAAATAAAGCT-3' primers. Both proteins were expressed using Bl21 *E. coli* strain following overnight induction at 16°C by adding 0.4 mM IPTG and purified with Ni^{2+}-NTA (Qiagen) followed by heparin and size-exclusion (GE Healthcare) chromatography columns.

Archaeal family-B DNA polymerase from *Thermococcus gorgonarius* (Tgo PolB exo-) used in control primer extension reactions on synthetic substrates containing UV induced DNA lesions was purified as described previously (Evans et al., 2000). The human DNA polymerase ε holoenzyme was kindly provided by Professor Juhani Syväoja (University of Eastern Finland, Finland).

Fluorescent primer template based assays

The HPLC grade DNA oligomers used to prepare synthetic primer-template substrates were purchased from ATDbio (Southampton, UK). The DNA oligomer containing pyrimidine-pyrimidone (6-4) photoproduct was kindly provided by Professor Shigenori Iwai (Osaka University, Japan). Primers contained a 5' Hex fluorophore label. Primer and template sequences are detailed in supplementary Table 1.

All the primer extension assays were performed at 37ºC as described previously (Jozwiakowski and Connolly, 2011). The typical primer extension reaction was performed in 20 µl volume containing 10 mM Bis-Tris-Propane-HCl, pH 7,0, 10 mM NaCl, 10 mM $MgCl_2$, 1 mM DTT, 20 nM primer-template substrate, 200 µM dNTP's (Roche) with 50 nM recombinant human PrimPol. The products of the primer-template extension reactions were monitored over time course of 2, 5, 10, 15 minutes. All single incorporation assays were performed in present of single dNTP and reactions were quenched after 30 minutes incubation.

Control primer extension with Tgo-PolB exo- were performed at 50ºC in 20 µl volume containing 20 mM Tris-HCl, pH 8,5, 20 mM NaCl, 2 mM MgSO4, 20 nM primer-template substrate, 100 µM dNTP's (Roche)

with 50 nM recombinant Tgo PolB exo-. Control primer extension with human Pol ε were performed in 20 µl volume containing 10 mM Bis-Tris-Propane-HCl, pH 7,0, 10 mM NaCl, 10 mM $MgCl_2$, 1 mM DTT, 20 nM primer-template substrate, 200 µM dNTP's (Roche) with 100 nM human DNA polymerase ε. The products of the primer-template extension reactions were monitored over time course of 2, 5, 10, 20 minutes.

Fluorescent primase assay

The non-radioactive primase assay was performed in three steps. Typically detection of primase activity was started from incubation of 1µM of the tested enzyme or 2 U of klenow-Taq (negatve control for the assay; purified as described in Engelke et al., 2000) in 20 µl reaction volume containing 500 nM ssDNA synthetic template (dAx60, dCx60, dGx60, dTx60) with a biotin modification at the 5' end, 500 µM rNTPs (Invitrogen) or 500 µM dNTPs (Roche), 10 mM Bis-Tris-Propane-HCl pH7, 10 mM $MgCl_2$, 50 mM NaCl. Primer synthesis was carried out for 2 hours at 37^{o}C then reaction supplemented with 0.2 U of kTaq and 15 µM FAM-6-dATP (Jena-Biosciences) and incubated at 37^{o}C for 45 minutes to allow fluorescent labeling of *de novo* synthesised primers. The primer synthesis/labeling enzymatic reactions were terminated by adding 450 µl of binding-washing (B-W) buffer (10 mM Tris-HCl 8.0, 500 mM NaCL, 10mM EDTA). The quenched reactions were added to ~30 µl of streptavidin coated beads (500 µl total volume) and mixed on a spinning wheel for 1 hour at 4^{o}C. After capturing the ssDNA templates, the suspension were spun down briefly to sediment the beads. The supernatant was removed and the beads were washed three times with 1 ml volumes of B-W buffer. The beads were then suspended in 20 µl of 8 M UREA 10 mM EDTA and boiled for 3 minutes in order to liberate primers. The 20 µl samples were spun down briefly, loaded on 15% polyacrylamide / 7M urea gel and resolved for 1h45min at 17watts. After electrophoresis gels were scanned for fluorescent signal and products of reaction/labeling of de novo synthesised primers were visualised.

Generation of a stable inducible cell line

Flp-In™ T-REx™ HEK-293 cells (Invitrogen) were used to make a stable cell line with inducible expression of epitope tagged PrimPol. Prior to transfection, cells were grown in 100 µg/ml Zeocin (Invitrogen) and 15 µg/ml Blasticidine (Invitrogen). Cells were seeded in a 6-well plate 24 hours after transfection with pcDNA5/FRT/TO plasmid encoding PrimPol-FlagStrep or PrimPol-HA, and pOG44 plasmid with Lipofectamine 2000 according to the manufacturer's instructions. 48 hours after, cells were split into 10 cm dishes and 72 hours after 15 µg/ml Blasticidine and 100 µg/ml Hygromycin (Invitrogen) added. Selective medium was replaced every 3-4 days until clones appeared visible and stocks made.

Immunofluorescent analysis

Cells were grown on coverslips, which for HEK-293 Flp-InTM T-RExTM cells were poly-L-lysine coated. Following siRNA transfection and/or DNA damaging treatments and recovery time, cells were either fixed directly in 3% paraformaldehyde (in PBS) for 15 minutes or pre-extracted by washing in 0.5% Triton X-100 in PBS before fixing. Cells were permeabilised with 0.2% Triton X-100 in PBS for 10 minutes, blocked with 3% BSA in PBS before immuno-staining steps. Coverslips were mounted on slides with Prolong Gold anti-fade (Invitrogen). Slides were analysed on a widefield Deltavision microscope for images, and a Nikon E400 for counting.

Antibodies used were anti-PrimPol 1:200 (in house), anti-RPA2 1:200 (Cell Signalling), anti-RAD51 1:400 (Abcam). Secondary antibodies were Alexa Fluor 488 goat anti-rabbit 1:2000, and Alexa Fluor 594 goat anti-mouse 1:2000. Cells were incubated with 250 nM Mitotracker Deep Red (final concentration) (Invitrogen) for 30 minutes prior to fixation. Immunolabeling of DNA fibers was performed with anti-rat BrdU (abcam) 1:1000, anti-mouse BrdU (Becton Dickinson) 1:500 and secondary Alexa Fluor 488-labeled anti-rat and Alexa Fluor 594-labeled anti-mouse (Invitrogen) both 1:250.

Cellular fractionation

Cellular fractionation protocol was modified from (Kannouche et al., 2004; Zlatanou et al., 2011). Cell pellet was resuspended in cytoskeletal (CSK) buffer (100 mM NaCl, 300 mM sucrose, 3 mM MgCl2, 10 mM Pipes (pH 6.8), 1 mM EGTA, 0.2% Triton X- 100) supplemented with protease and phosphatase inhibitors (Roche), and incubated on ice for 5 minutes and then spun in a cold centrifuge for 10 minutes at 13,000 rpm. The supernatant was collected as the soluble fraction, and the insoluble pellet was twice PBS washed before resuspended and boiled in Laemmli sample buffer. For further fractionation the insoluble pellet was resuspended in CSK buffer with 50 mM NaCl and 1 µl/ml Benzonase, at room temperature for 20 minutes with occasional agitation, before centrifugation. The soluble fraction was retained and the insoluble fraction boiled in Laemmli sample buffer. Whole cell extracts were prepared by lysing cells in NETN buffer (150 mM NaCl, 50 mM Tris (pH 7.5), 5 mM EDTA, 0.5% NP- 40), and incubated on ice before sonication and determining protein concentration.

Generation of PrimPol knockout cell lines in avian DT40 cells

Construction of targeted vectors containing antibiotic resistance cassette was performed via gateway cloning system (Iiizumi et al., 2006) and the primers used summarized in Supplementary Table 2. DT40 cells were electroporated and clones selected as described previously (Sonoda et al., 1998) using histidinol

and puromycin (Sigma) respectively at 1 mg/ml and 0.5 mg/ml. Resistant clones were screened for alleles disruption via Southern blot analysis and RT-PCR using superscript one step kit (Invitrogen), with primers summarized in Supplementary Table 3. Human PrimPol cDNA was sub-cloned into TET inducible vector (adapted from Clontech in Takeda's laboratory, Kyoto University, Japan) containing luciferase gene reporter for clone selection.

DT40 cells were grown at 39°C in RPMI 1640 medium supplemented with 10^{-5} M β- mercaptoethanol, penicillin, streptomycin, 10% foetal calf serum and 1% chicken serum (Sigma), and counted manually on haemocytometer with trypan blue (Invitrogen) staining to assess growth defect. Cell cycle analysis was determined by BrdU labelling and flow cytometry analysis as described previously (Hégarat et al., 2012). Cell viability assay was performed using CellTiter-Blue (Promega) following manufacturer's instructions.

DNA fiber spreading and post replication repair assay

Both techniques were performed as previously described (Edmunds et al., 2008). Post replication repair protocol was adapted to measure DNA replication rate during unperturbed DNA replication and following UV-C irradiation, by pre-labeling cells with ^{14}C-thymidine over two doubling time to normalize the amount of total DNA, and by pulse labeling the cells for 20 minutes with tritium thymidine.

Xenopus egg extract preparation and assays

Demembranated sperm nuclei were prepared by lysolecithin treatment as previously described (Murray et al., 1991). For preparation of interphase Xenopus egg extracts, unfertilized eggs were dejellied, washed and activated with the calcium ionophore A23187 as previously described (Kubota and Takisawa, 1993). Activated eggs were washed in extraction buffer (XB: 10 mM Hepes-KOH, pH 7.7, 100 mM KCl, 0.1 mM $CaCl_2$, 1 mM $MgCl_2$, 50mM sucrose) at 4°C, and then, following removal of excess buffer, crushed by centrifugation at 15,000 x g for 10 minutes. The cytoplasmic layer was supplemented with aprotinin (10 µg/ml), cytochalasin B (50 µg/ml), creatine phosphate (30 mM) and creatine phosphokinase (150 µg/ml) then centrifuged at 60,000 x g 10 min, 4°C (Beckman Optima TLA-55) to generate the replication-competent supernatant fraction. Chromatin isolation was carried out using the method of (Errico et al., 2007) and recombinant GST-geminin prepared as previously described (Stokes and Michael, 2003). PCNA and MCM7 antibodies were both from AbCam while Cdc45 antibody was a generous gift of Vincenzo Costanzo (CRUK Clare hall) and Orc1 antibody, from Dr Julian Blow (Dundee University).

Targeting of the PrimPol locus in mouse ES cells

The *PrimPol* (*CCDC111*) knock out first targeting construct was generated using standard pRed/ET recombineering methods in the IRB Mutant Mouse Core facility. Briefly, the genomic locus of *PrimPol* was captured from a BAC clone (bMQ227f06, Sanger Institute) and screened by PCR. Zeo/pheS and LoxP flanked EM7-Kanamycin cassettes were sequentially recombineered into the BAC up and downstream of exon 5, that contains critical enzymatic residues (AEP I domain), and the modified genomic locus recombineered into a capture vector. The EM7-Kanamycin cassette was deleted by Cre expression, leaving a single LoxP site 3' of exon 5. A Gateway reaction was then carried out to swap the Zeo/pheS cassette for a LacZ/Neo Trap cassette containing a LoxP site upstream of exon 5 (ENSMUSE00001229433) (Supplemental Figure S4C). ES cells were targeted by electroporation of an AsiSI linearized construct followed by selection with Neomycin. Positive clones (*PrimPol*$^{+/trap}$) were screened by long range PCR using DNA isolated from targeted ES cell clones as substrate and Southern blotting was used to confirm single insertion (details available upon request).

Generation of PrimPol deficient mice

Positive *PrimPol*$^{+/trap}$ clones were injected into 3.5 day old mouse blastocysts derived from C57B6/j mice. Approximately 12-15 ES cells were injected into each blastocyst, and injected blasts were re-implanted back into the oviduct of 2.5 day old pseudo-pregnant foster mice. Chimeras born from these injections were scored for chimerism by coat color analysis, and the chimeras showing the highest contribution from the ES cells were mated with C57B6/j wild-type mice. Agouti offspring obtained from these test-matings were screened for the presence of the mutation by PCR. Mice positive for the allele were bred to FlpO (C57BL/6J-Tg(Pgk1-FLPo)10Sykr/J , Jackson Laboratories) transgenic mice to delete the genetrap and generate the floxed allele, *PrimPol*^{cond} (Supplemental Figure S4C). These animals were subsequently bred to Sox2-Cre (Tg(Sox2-cre)#Amc/J , Jackson Laboratories) transgenic mice to delete exon 5 generating the knockout allele, *PrimPol*$^{-}$ (Supplemental Figure S4C). Phenotypic analysis of animals will be described elsewhere. Mice were maintained on a mixed 129/B6 background and all animals were handled in strict accordance with the guidelines of the European Community (86/609/EEC) at the animal facilities in the Barcelona Science Park. The protocols were approved by the Animal Care and Use Committee of the Barcelona Science Park (IACUC; CEEA-PCB) in accordance with applicable legislation (Law 5/1995/GC; Order 214/1997/GC; Law 1201/2005/SG). All efforts were made to minimize suffering.

Generation of mouse embryo fibroblasts lacking PrimPol expression

Mouse embryonic fibroblasts (MEFs) were isolated from *PrimPol*$^{+/-}$ pregnant females at E14.5. Uterine horns were removed and washed with PBS. Embryos were removed and decapitated. Viscera was removed and tail tissue was taken for PCR genotyping (details available upon request). Embryos were washed in fresh PBS and incubated over night at 4ºC in 5ml trypsin/EDTA. Selected embryos were incubated in trypsin at 37ºC for 20 minutes and physically disaggregated by pipetting in Dulbecco's modified Eagle Medium (DMEM) with 10% fetal bovine serum (FBS), 2mM L-glutamine and 100 U/ml penicillin/streptomycin (MEF media). Supernatant containing disaggregated cells was plated and washed the following day to remove non-adherent cells. MEFs were cultured in MEF media and were used prior to passage 5 for experiments.

Real time PCR analysis of *PrimPol* mRNA levels

To determine relative mRNA levels of PrimPol, a quantitative Real Time-PCR (qRT-PCR) was developed for the mouse *PrimPol* gene. qRT-PCR was performed using the Step-One-Plus Real Time PCR System (Applied Biosystems) and SYBR Green PCR Master Mix (Applied Biosystems) following manufacturer's instructions. Relative levels were calculated using the comparative CT method. For PrimPol, a forward primer in Exon 5 (taacaaattggccaacccaggag) and a reverse primer in exon 7 (accttagcttcatcatcctcggc) were used. A diagram of the strategy and results run on an agarose gel with a 100 bp size ladder are shown (Supplemental Figure S4D and E). Real time PCR reactions to determine relative levels were performed in triplicate and GAPDH was used as an endogenous control for normalization (Supplemental Figure S4F).

Metaphase chromosome preparations

Mitotic MEF populations were enriched by colcemid ($2x10^{-7}$M) treatment for 1 to 2 hours. Cells were harvested by trypsinization, osmotically swollen with 0.075M KCL for 15 minutes at 37ºC and fixed with ice cold methanol:glacial acetic acid (3:1) added dropwise. Cells were resuspended in 300ul of fixative and 30ul was spread over a glass slide that was then inverted over an 80ºC water bath for 7 seconds and dried on the hot lid. Slides were stained in 5% Giemsa solution for 10 minutes and examined under oil immersion at 63X-100X magnification, using a white light source. A minimum of 50 spreads was counted per sample and the number of chromosomes per spread and aberrations per spread were recorded. Aphidicolin (Sigma) treatment was performed on primary MEFs cultured in MEF media containing 300 nM aphidicolin for 36 hours.

SUPPLEMENTARY REFERENCES

Engelke, D. R., Krikos, A., Bruck, M. E., and Ginsburg, D. (1990). Purification of *Thermus aquaticus* DNA polymerase expressed in *Escherichia coli*. Anal. Biochem. *191*, 396-400.

Errico, A., Costanzo, V. & Hunt, T. (2007). Tipin is required for stalled replication forks to resume DNA replication after removal of aphidicolin in Xenopus egg extracts. Proc. Natl. Acad. Sci. *104*, 14929-14934.

Evans, S.J., Fogg, M.J., Mamone, A., Davis, M., Pearl, L. H. & Connolly, B.A. (2000) Improving dideoxynucleotide-triphosphate utilisation by the hyper-thermophilic DNA polymerase from *Pyrococcus furiosus*. Nucleic Acids Res. *28*, 1059–1066.

Iiizumi, S., Nomura, Y., So, S., Uegaki, K., Aoki, K., Shibahara, K., Adachi, N., & Koyama, H. (2006) Simple one-week method to construct gene targeting vectors: application to production of human knockout cell lines. BioTechniques *41*, 311-316

Hégarat, N., Smith, E., Nayak, G., Takeda, S., Eyers, P. A., & Hochegger, H. (2012). Aurora A and Aurora B jointly coordinate chromosome segregation and anaphase microtubule dynamics. J. Cell Biol. *195*, 1103-13.

Jozwiakowski, S. K., & Connolly, B. A. (2011). A modified family-B archaeal DNA polymerase with reverse transcriptase activity. Chembiochem *12*, 35-7.

Stokes, M. P., & Michael, W. M. (2003). DNA damage-induced replication arrest in Xenopus egg extracts. J Cell Biol. *163*, 245-55.

Zlatanou, A., Despras, E., Braz-Petta, T., Boubakour-Azzouz, I., Pouvelle, C., Stewart, G. S., Nakajima, S., Yasui, A., Ishchenko, A. A., Kannouche, P. L. (2011). The hMsh2-hMsh6 Complex Acts in Concert with Monoubiquitinated PCNA and Pol eta in Response to Oxidative DNA Damage in Human Cells. Mol. Cell *43*, 649–662.